POLITECNICO DI MILANO

Facoltà di Ingegneria dei Processi Industriali

Dipartimento di Chimica, Materiali e Ingegneria Chimica

“Giulio Natta”

FREE-RADICAL POLYMERIZATION KINETICS SOLVED BY RIGOROUS COMPUTATION

RELATORE: Prof. Dr. Massimo MORBIDELLI

Edoardo MELLONI 783455

Anno Accademico 2013 – 2014

A mia madre Tiziana e a mio padre Fabio, senza i quali tutto ciò che ho potuto fare fino ad ora non sarebbe stato possibile.

A mio nonno Ernesto che sicuramente avrebbe voluto essere qui questo giorno.

A Luna, per essere sempre stata al mio fianco.

Acknowledgements

Grazie ai miei più cari amici che hanno accompagnato il mio percorso universitario negli ultimi 6 anni, compresi i 2 anni in Brasile: Sà, Paolone, Paolino, Toni, Dico, Ale A., Ale C., Ale S., Dave e Andre.

Grazie alla Banda Bagaj, terrore di tutte le squadre di scapoli ed ammogliati milanesi.

Grazie agli amici che, anche dopo i tanti anni di lontananza da Roma, rimangono persone importanti su cui so di poter sempre contare: Cagne, Pedro, Blanc, Lodo, Mary, Ale I., Giu C. e Giu M.

Grazie ad Amina, amica e fagiana che c'è sempre stata e sempre ci sarà, a prescindere dall'angolo di mondo in cui staremo.

Grazie all'ex Dindelli, compagni di squadra e amici che hanno reso il mio ultimo anno a Milano il più bello.

Grazie Marino e Alfredo perché siete stati tra i primi amici conosciuti a Milano e perché, nonostante si siano prese strade diverse, è sempre bello ritrovarvi.

Grazie al Siwa, perché è il Siwa.

Grazie a Giulia P., amica nel mio ultimo anno in Brasile, compagna di viaggio ed elemento insostituibile nelle pizzate. L'unica che mi capisce a briscola chiamata.

Grazie a Beatriz, a amiga com quem mais briguei, et grazie à François (autrement dit Fransuá): abonnés à nos pizzas et composants essentiels de notre groupe du vendredi-et-samedi-soir.

Grazie a Lucas e Esmar, amigos que me suportaram todo ao longo da minha permanência no Brasil.

Grazie a equipe de atletismo da poli, com a qual passei muitas horas e muitos dias de treino durante quase dois anos, compartilhando muita alegria.

RIASSUNTO

La distribuzione dei pesi molecolari (DPM) di un polimero influenza le proprietà meccaniche, termiche e reologiche del materiale. Inoltre, l'analisi in tempo reale di una reazione di polimerizzazione è un compito complicato e, di conseguenza, i procedimenti di controllo devono basarsi su valori generati dai modelli. Per questo motivo, è di fondamentale importanza possedere dati affidabili sulle distribuzioni dei pesi molecolari, migliorare l'efficienza dei metodi esistenti e svilupparne di nuovi capaci di prevedere le eterogeneità delle reazioni di polimerizzazione. Sperimentalmente, la DPM può essere ottenuta usando tecniche come la cromatografia a permeazione di gel.

Per predire la DPM, negli ultimi decenni si sono sviluppati diversi metodi. Uno dei principali è quello dei momenti statistici, basato su concetti puramente statistici, che non riescono a descrivere completamente la DPM. Oltre a questo metodo, vi sono le approssimazioni col metodo di Galerkin, che usano polinomi ortogonali – nel caso specifico polinomi di Laguerre – cui coefficienti sono calcolati utilizzando i momenti statistici; la distribuzione è ottenuta risolvendo un numero di equazioni definito dall'utente, relazionato alla precisione desiderata. Per ultimo, si può adoperare il metodo delle funzioni generatrici di probabilità per prevedere le DPM, ma ciò necessita di un'inversione della trasformata di Laplace, che introduce problemi numerici non sempre risolvibili.

Nel presente studio si è risolto il sistema rigoroso di equazioni differenziali ordinarie, con l'obiettivo di ridurre le imprecisioni e le limitazioni introdotte dalle approssimazioni. L'ottenimento diretto della DPM completa richiede la risoluzione di un sistema che contiene circa dalle $2N_{max}$ alle $3N_{max}$ equazioni differenziali ordinarie *stiff*, compito che fino a qualche anno fa non era possibile affrontare a causa delle limitazioni associate alla capacità di calcolo. Si è modellata la DPM per una reazione di polimerizzazione radicalica libera di stirene e di metacrilato di metile. Un'attenzione particolare è stata data alla velocità di terminazione che è, al momento, uno degli argomenti più studiati nella polimerizzazione via radicali liberi. I risultati delle simulazioni sono stati confrontati con i dati sperimentali ottenuti da reattori convenzionali e, successivamente, con dati sperimentali provenienti da un millireattore non convenzionale.

Parole-chiave: Polimerizzazione radicalica libera. Distribuzione de pesi molecolari. Effetto Gel. Effetto Norrish–Trommsdorff. Integrazione diretta.

ABSTRACT

It is well known that the molecular weight distribution (MWD) of a synthetic polymer affects its mechanical, thermal and rheological properties. Furthermore, the on-line analysis for polymerization reaction is a difficult task and, consequently, the control procedures must rely on values given by models. As such, it is extremely important to have reliable data on the MWD, improve the efficiency of existing methods and develop new ones to predict the heterogeneities of polymerization reactions. Experimentally, the MWD can be obtained using techniques such as Gel Permeation Chromatography (GPC).

To predict the MWD, many methods have been developed over the last decades. One of the main methods is the statistical moment treatment, which is based on a pure statistical concept and do not describe the whole MWD. Moreover, Galerkin approximation uses orthogonal polynomials -in general Laguerre polynomials- whose coefficients are calculated exploiting the statistical moment definition and the distribution is generated by solving a user-defined number of equations based on the desired precision. Finally, probability-generating functions that have been used to predict MWDs require Laplace transforms inversions, introducing numerical issues that must be bypassed and are not always solvable.

It has been decided to base the approach without adopting any of these methods but directly solving the rigorous ordinary differential equation (ODE) system in order to reduce the inaccuracies and the limitations introduced by approximations. The direct obtention of the MWD requires the resolution of a system containing approximately $2N_{max}$ up to $3N_{max}$ stiff ODE equations that, a few years ago, was unfeasible due computational time limitations. The MWDs for a free radical styrene polymerization system and a methyl methacrylate system have been modeled. A special focus was given to the termination rate constant, which is, at the present, one of the most investigated topics in free radical polymerization. The results of the simulations were compared to experimental data taken from conventional reactors and, subsequently, to experimental data coming from an unconventional millireactor.

Keywords: Free-radical polymerization. Molecular weight distribution. Gel effect. Norrish–Trommsdorff effect. Polymer science. Direct integration.

Chapter 1. Introduction to Polymer Science

1.1. Polymers characterization

Polymers are macromolecules composed by the repetition of a basic unit, called monomer (ODIAN, 2004). The characterization of polymeric materials can be done over a variety of levels, depending on the utility of the concerned material. Properties such as strength, thermal stability, resistance and impermeability are of great interest (ODIAN, 2004). In order to estimate these properties it is usual to determine the molecular mass of a polymer, its molecular structure (linear or branched) and its thermal and mechanical properties.

1.1.1. Molecular weight distributions

The molecular weight is a crucial characteristic of a polymer because many physical properties depend on it. Among the properties that are strongly related to the molecular weight one can find stiffness, toughness, strength and viscosity (INDIAN ACADEMY OF SCIENCES). In general a low molecular weight leads to poor mechanical properties and excludes the material from any commercial application.

A polymerization reaction leads to a heterogeneous product; there is not a single molecular weight for a polymerization product but rather a molecular weight distribution (MWD). The physical properties may then be expressed as a function of the MWD. In order to keep things simple it is possible to define some types of average molecular weights that can be used to describe some properties, neglecting the rigorous MWD of the polymer.

Figure 1-1 Schematic plot of a molecular weight distribution with the values of various average molecular weights

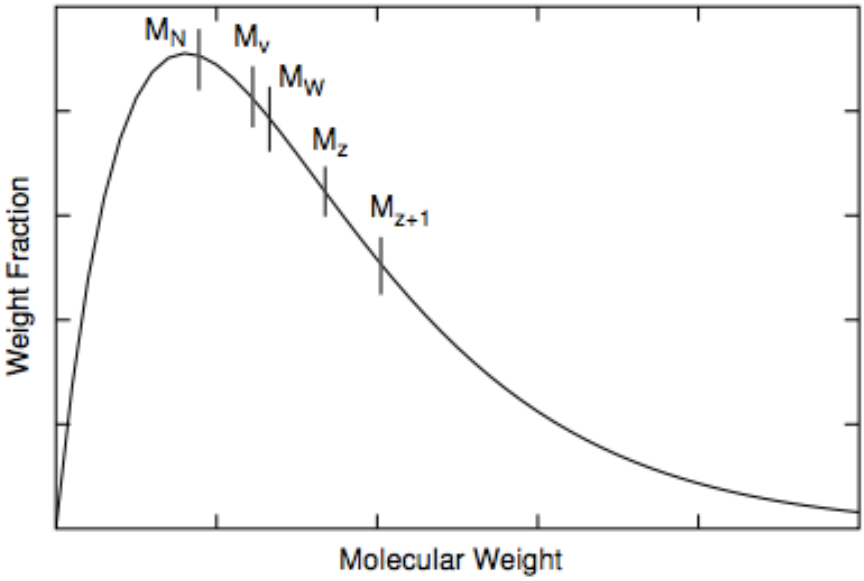

Source: (LUCAS; SOARES; MONTEIRO, 2001)

1.1.1.1. Number average molecular weight

The number average molecular weight M_N is used to describe properties such as boiling point elevation (colligative properties) that depend only on the number of molecules present and are not significantly influenced by the size of the particles itself (http://www.polymersdatabase.com/).

Let N_i be the number of molecules with molecular weight M_i, then the number average molecular weight is expressed as it follows:

$$\boldsymbol{M_N = \frac{\sum_{i=1}^{\infty} N_i M_i}{\sum_{i=1}^{\infty} N_i}} \qquad \textbf{Eq. 1}$$

Physically, it is the total weight of polymer dived by the number of polymer molecules. An alternative form of this parameter is:

$$\boldsymbol{M_N = \frac{1}{\sum_{i=1}^{\infty} \frac{w_i}{M_i}}} \qquad \textbf{Eq. 2}$$

This represents the same parameter written in terms of weight fraction of polymers with molecular weight M_i, denoted as w_i.

1.1.1.2. Weight average molecular weight

When a property is no longer dependent on the number of molecules but also by their relative length or weight, a new parameter needs to be introduced (ODIAN, 2004). The weight average molecular weight M_W is obtained by replacing - in the number average molecular weight formula - the number of polymers having molecular weight i, N_i by the weight of polymers having molecular weight *i*, N_iM_i:

$$\boldsymbol{M_W = \frac{\sum_{i=1}^{\infty} N_i M_i^2}{\sum_{i=1}^{\infty} N_i M_i}} \qquad \textbf{Eq. 3}$$

1.1.1.3. Polydispersity index

As it can be seen in Figure 1-1, the MWD resembles a probability distribution curve. The standard deviation is a parameter that characterizes the spread of any distribution function and, in the case of a polymerization reaction we can define a simple parameter which describes how large is the MWD function (ODIAN, 2004). The polydispersity index P_D uses the average molecular weights previously described and it is defined as it follows:

$$\boldsymbol{P_D = \frac{M_W}{M_N}} \qquad \textbf{Eq. 4}$$

By definition $M_W \geq M_N$, consequently $P_D \geq 1$. When the polydispersity index is one the distribution is said to be monodisperse. In general, all real polymers have the polydispersity index greater than one (MATYJASZEWSKI; DAVIS, 2003) and this describes the distribution width.

1.1.2. Molecular weight measurements

Several techniques can be used to determine these parameters; the most common methods are viscosimetry, light scattering techniques and size exclusion chromatography (KIRSHENBAUM, 1973).

1.1.2.1. Viscosimetry

The viscosity describes a fluid's internal resistance to flow. It is a measure of the resistance of a fluid to deformation under shear stress. Due to entanglements of the large macromolecules, the viscosity of a liquid increases when a polymer is dissolved into it (MILLER-CHOU; KOENIG, 2003). Many methods are available to measure the viscosity of a polymer solution; one of these is the Ostwald method, in which the unknown viscosity of a liquid is determined by comparison with a known viscosity. The molecular weight obtained with this technique is called viscosity average molecular weight and differs from the average molecular weights previously discussed (section 1.1.1.1 and 1.1.1.2).

1.1.2.2. Dynamic light scattering

The dynamic light scattering (DLS) is able to determine the size distribution profile and consequently the MWD of polymers in solution. Rayleigh scattering occurs when light hits small particles if they are small enough compared to the wavelength (BERNE; PECORA, 2000). The intensity of the scattered light suffers a time-dependent fluctuation related to the Brownian motion of the molecules in solution. Information about the movement time scale of the scatterers (elements causing the scattering phenomenon) is contained within this intensity fluctuation which, in turn, is relatable by means of a function to the particles' size (EDWIN, 2001).

1.1.2.3. Gel permeation chromatography

The gel permeation chromatography (GPC) is a type of size exclusion chromatography commonly used to characterize polymers. The equipment is based on a column filled with a stationary phase made of a packed porous bed. A mobile phase containing the polymer to be analyzed dissolved in an appropriate solvent is pumped inside the column and flows through the porous bed. The smaller molecules (low molecular weights) can easily enter the pores and will consequently spend more time inside the column. The

molecules having high molecular weights will not enter the pores and will then be the first to leave the column (SKOOG; HOLLER; NIEMAN, 2007).

A detector is placed at the exit of the column and can be a concentration sensitive detector (such as refractive index detector) or/and a molecular weight sensitive detector (like a multi angle light scattering detector).

The resulting chromatogram is a MWD as a function of retention time or volume.

Chapter 2. Bibliography Review

In Chapter 1 the principal average molecular weights have been discussed. However, many mechanical properties of a polymer depend on the complete MWD and the averages of the distribution are not sufficient in order to exhaustively describe those properties. The interest in having a complete MWD is efficiently summarized by Crowley and Choi (1998, p. 1017) who used, as an example, properties such as impact resistance and tensile strength: "[...] if a quantitative relationship between the MWD and a polymer property exists, it should be possible to indirectly control the property of interest by controlling the MWD during polymerization reactor operation". This idea also introduces the concept of a rapid computation just as much as precise and efficient.

In fact, as long as the computer processors are becoming more powerful, there is great interest on developing models even more accurate and complete. Accuracy and completeness do not refer only to the prediction of the final reaction parameters such as conversion, M_N or M_W but also to the correct prediction of the conversion trend as well as the MWD for each instant of reaction. The reason is that an on-line analysis for polymerization reactions is a difficult task and, consequently, the control procedures must rely on values given by models (ASUA, 2007). As a matter of fact, it is not before 1998 that a study on on-line monitoring of polymerization reactions was published (FLORENZANO; STRELITZKI; REED, 1998). Although 16 years have passed since then, the task still present high lag times, typically up to 100 seconds (REED, 2014) and the information obtained in this time is limited to the evolution of conversion, M_N, M_W and viscosity and phenomena like microgelation or microcrystallization.

Moreover, a complete MWD contains information about the kinetic process that led to the final polymer. It is "a record of the kinetic history of the reactions which occurred during its formation" (CLAY; GILBERT, 1995). Thus, an accurate and complete MWD can provide the kinetic constants estimation of the free radical polymerization reaction, contributing to a better understanding of the mechanisms behind the polymer formation and their relative importance.

2.1. Polymerization Kinetics

Depending on the reaction mechanisms the principal polymerization reaction families are step-growth and chain-growth polymerization systems (ODIAN, 2004). The step-

growth occurs when the monomeric molecule presents functional groups such as carboxyl, epoxides and hydroxide. The chain-growth involves an unsaturated monomeric unit which has double bonds or ring structure. The focus of this chapter will be on chain-growth polymerization systems. As an example, the styrene polymerization kinetic scheme can be taken into account: the reaction occurs through a multi-step mechanism that includes initiation, propagation, transfer and termination.

- Initiation

$$I \overset{k_d}{\rightarrow} 2R$$

$$R + M \overset{k_i}{\rightarrow} P_1$$

- Propagation

$$P_i + M \overset{k_p}{\rightarrow} P_{i+1}$$

- Transfer

$$P_i + S \overset{k_{fs}}{\longrightarrow} D_i + P_1$$

$$P_i + M \overset{k_{fm}}{\longrightarrow} D_i + P_1$$

- Termination

$$P_i + P_k \overset{k_{tc}}{\longrightarrow} D_{i+k}$$

$$P_i + P_k \overset{k_{td}}{\longrightarrow} D_i + D_k$$

Where I is an appropriate initiator, R is the initiator radical, M is the monomer, P is a macroradical polymer of length i, D is a dead polymer of length i and S is the solvent.

The initiation occurs when the bonds of a chemical compound containing labile groups (such as disulfides or peroxides) are broken, resulting in a species which can be ionic or radical, depending on the original initiator. A typical initiator for styrene polymerization is benzoyl peroxide. The monomer is then activated by reacting with the radical species produced in the bond cleavage of the initiator.

The propagation reaction occurs when the reactive end of a polymer chain interacts with a monomer, which results in a longest polymer and transfers the reactive site to its new end.

The chain transfer reaction transfers the active site of a polymer radical to the monomer, the solvent or a transfer agent intentionally added to the reacting system.

This kind of reaction produces a new monomeric radical and lowers the overall molecular weight of the final polymer.

Finally, the termination reaction occurs when two free radical polymers interact and terminate the polymerization process. The termination can be either by combination or by disproportionation. In the termination by combination a dead polymer is produced as a result of the interaction between two radical polymers while in the termination by disproportionation two dead polymers of the same length of the radical polymers interacting are produced.

2.1.1. Cage effect (ODIAN, 2004)

The chain initiation step of the reaction must consider inefficiencies of the system. A parameter called efficiency factor, f, is used to take into account these phenomena. Its theoretical value ranges from 0 to 1 - typically between 0.3 and 0.8 - and depends on:

- Primary recombination or cage effect

Figure 2-1 Primary recombination of Benzyl peroxide - brackets indicate that the reaction is happening within the solvent cage -

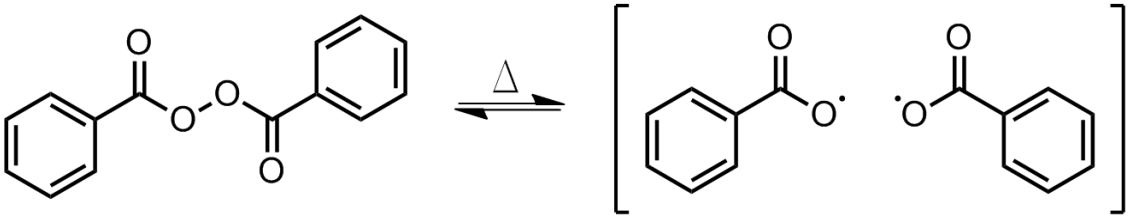

Source: (COWIE; ARRIGHI, 2007)

This happens when the initiator splits into two radical and neither of them leave the solvent cage but instead they recombine between them without initiating a new polymeric chain.

- Other side reactions such as secondary recombination, which is an initiator recombination outside the solvent cage.

2.1.2. Norrish–Trommsdorff effect (MATYJASZEWSKI; DAVIS, 2003)

The Norrish-Trommsdorff effect, also known as gel effect, is an auto-acceleration of the polymerization reaction at high monomer conversions. This effect has been observed in

reacting systems containing, for example, methacrylate or styrene. This phenomenon is related to the conversion dependence of the termination rate constant and it has been experimentally observed that, because of this, the termination rate constant sharply decreases, making the kinetic propagation step predominant. It only occurs in isothermal reactors being that the polymerization auto-acceleration due to temperature increase in non-isothermal reactors does not happens for the same reasons.

One explanation to the Norrish-Trommsdorff effect, which is also the most common explanation found in literature, links the termination kinetic rate constant diminution to the difficult diffusion of the macromolecules through the reaction mixture as long as the monomer conversion increases. Chain entanglements are the cause of the macroradicals reduced mobility, impeding their diffusion, thus lowering the termination rate constant k_t.

The different chemical nature of the monomers involved in the polymerization leads to a different behavior when considering the gel-effect. In fact, the Norrish-Trommsdorff effect is typically much more significant in the polymerization of MMA rather than in that of styrene. For this reason, many industrial polymerization processes are carried out in the presence of a solvent (KRICHELDORF; NUYKEN; SWIFT, 2010). In the MMA polymerization, the steps of the gel-effect clearly appear: at low conversion and low viscosities, the rate of termination is determined by segmental diffusion, which is – for short chain lengths – a relatively fast step. However, as long as the monomer conversion increases, the live polymers become longer and the viscosity increases, making the termination step slower and slower (BENSON; NORTH, 1962).

Figure 2-2 Depiction of the mechanisms involved in the termination process

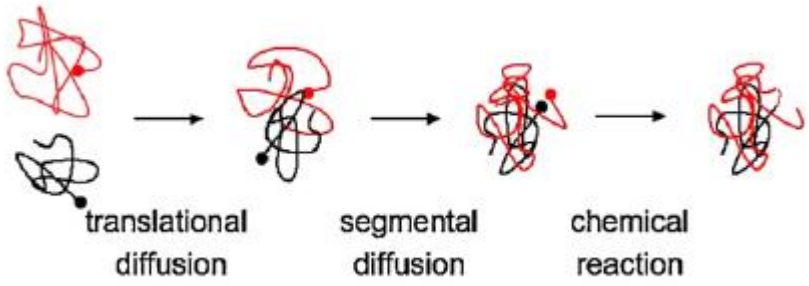

Source: (BARNER-KOWOLLIK; RUSSELL, 2009)

When leading with bulk polymerizations or with solution polymerizations at high monomer to solvent ratios this effect becomes very important.

During the last decades many studies tried to describe the isothermal diffusional limitations for the free radical polymerization of MMA. The models developed can be divided into three main groups: mechanistic, semi-empirical and fully empirical.

One empirical correlations based on experimental data is the one presented by Hui and Hamielec (1972):

$$g_t = \frac{k_t}{k_{t0}} = exp[-2(A\chi + B\chi^2 + C\chi^3)] \quad \textbf{Eq. 5}$$

$$A = 2.57 - 5.05 * 10^{-3}T$$

$$B = 9.56 - 1.76 * 10^{-2}T$$

$$C = -3.03 + 7.85 * 10^{-3}T$$

Where T is the temperature in Kelvin, χ is the monomer conversion and k_{t0} is the termination rate constant at zero monomer conversion.

The mechanistic models focus on the description of the dynamics of the entanglements between macromolecules (TULIG; TIRRELL, 1981) while the semi-empirical models use many different variations on the free volume theory (CHIU; CARRATT; SOONG, 1983) (MASCHIO; MOUTIER, 1989).

In such models the propagation and the termination rate constants variation is expressed as a function of a parameter:

$$k_p = k_{p0} g_p \quad \textbf{Eq. 6}$$

$$k_t = k_{t0} g_t \quad \textbf{Eq. 7}$$

Here k_{p0} and k_{t0} are the values of the rate constants at very low monomer conversion. Note that, for Eq.6, g_p remains equal to 1 except for extremely viscous conditions (SCHMIDT; RAY, 1981). This is due to the fact that the propagation step always involves a monomer which, regardless of the diffusional environment, has always a relatively high diffusivity. Ross and Laurence (1976) developed a bulk correlation based on the free volume theory. Later, Schmidt and Ray (1981) extended the correlation to solution polymerization:

$$g_t = \begin{cases} \left[\boldsymbol{if}\ \boldsymbol{V_f} > \boldsymbol{V_{fcr}}\right] 0.10575 exp\left[17.15V_f - 0.01715(T - 273.2)\right] \\ \left[\boldsymbol{if}\ \boldsymbol{V_f} \leq \boldsymbol{V_{fcr}}\right] 2.3 \cdot 10^{-6} exp(75V_f) \end{cases}$$

$$V_{fcr} = 0.1856 - 2.965 \cdot 10^{-4}(T - 273.2)$$

$$V_f = V_{fp}\varphi_p + V_{fm}\varphi_m + V_{fs}\varphi_s$$

$$V_{fp} = 0.025 + \alpha_p(T - T_{gp})$$

$$V_{fm} = 0.025 + \alpha_m(T - T_{gm})$$

$$V_{fs} = 0.025 + \alpha_s(T - T_{gs})$$

where φ_p, φ_m and φ_s are the volume fraction of polymer, monomer and solvent respectively. α_p, α_m and α_s are the coefficients of volumetric expansion and T_{gp}, T_{gm} and $T_{gs}$are the glass transition temperatures.

Figure 2-3 shows the gel effect at various monomer concentrations. At low monomer concentrations (20% and 40% v/v.) the conversion profile is smooth without any considerable change. At higher concentrations (60%, 80% v/v. and bulk) two distinct reaction steps are distinguished:

- At the beginning, the concentration profile is smooth, the conversion is low and the viscosity of the solution is still low.
- As long as the conversion increases, the viscosity of the solution increases, thus lowering the termination step regulated by the segmental diffusion. The concentration of the radicals in the reaction mixture increases, thus promoting the propagation step and, consequently, a rise in the conversion profile is observed.

Figure 2-3 Data for MMA polymerization in benzene at 50°C, [BPO]=10 g/L. (1) [MMA] bulk. (2) [MMA]=80%v/v. (3) [MMA]=60%v/v. (4) [MMA]=40%v/v. (5) [MMA]=20%v/v

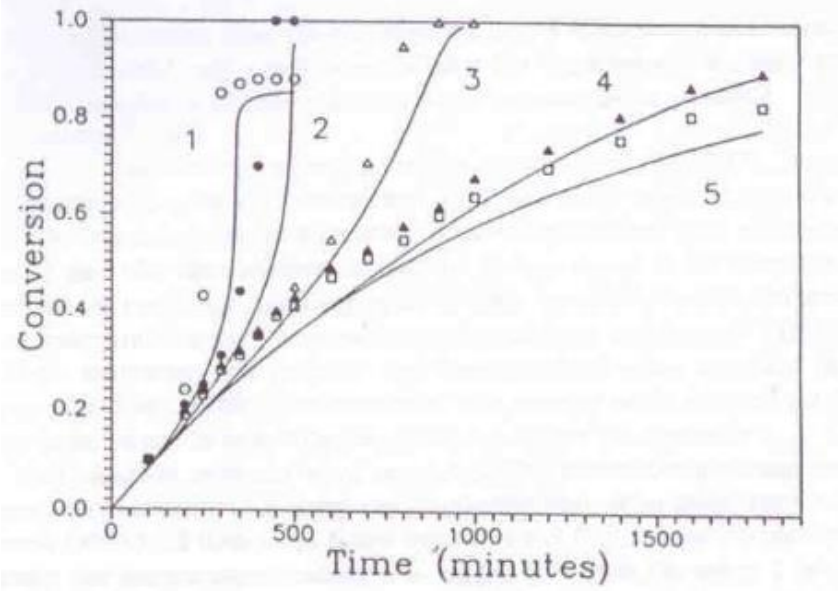

Source: (SCHULTZ; HARBORTH, 1947).

Figure 2-3 clearly shows that, in the case of the MMA polymerization, the dilution of the system strongly influences the diffusion of the radical macromolecules.

It is possible to see the impact of the gel effect over the monomer conversion in the Figure 2-4.

Figure 2-4 Conversion evolution along time in a Methyl Methacrylate (MMA) reacting system

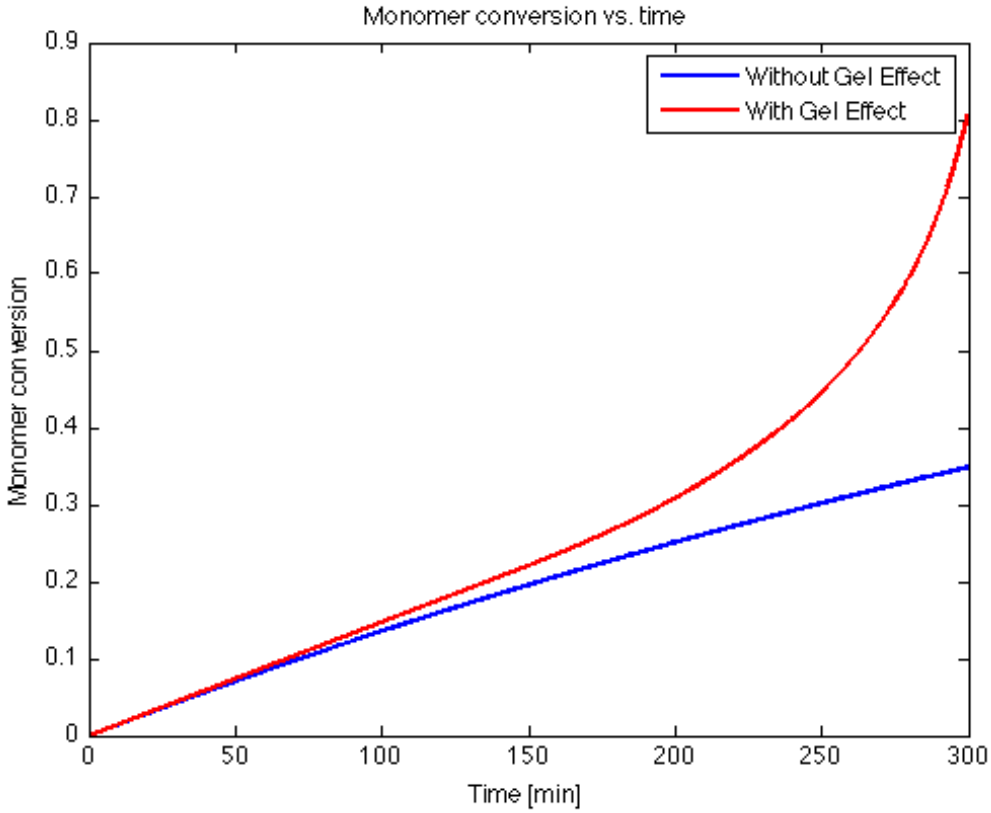

Source: (MELLONI, 2014)

As shown in Figure 2-4 there is a huge difference in considering or not this kinetic constant reduction and this will be an important step of this work.

2.2. Non-Rigorous computation methods for MWDs

Due to the reduced computational capacity of the old processors, the direct numerical integration of the polymerization kinetic equations was an impossible task. In literature (SARMORIA; ASTEASUAIN; BRANDOLIN, 2012) (PLADIS; KIPARISSIDES, 1998) it is possible to find various methods - besides the direct resolution of the ordinary differential equations (ODE) system, which is generated by the material balances applied to all the involved species- to compute a complete (or almost complete) MWD for a free radical polymerization system. The most significant available methods can be divided into:

- Statistical moment method
- Laplace transform methods
- Interval splitting

- Galerkin approximation.

Here follows a review of these methods.

2.2.1. Statistical moment method

In some situations the statistical moment method is a very efficient way to describe properties of a polymer distribution. The statistical moment of a given distribution is defined as:

$$\boldsymbol{\lambda_k(t) = \sum_{s=1}^{\infty} s^k P_s(t),\ k = 0, 1, \ldots} \qquad \textbf{Eq. 8}$$

$$\boldsymbol{\mu_k(t) = \sum_{s=1}^{\infty} s^k D_s(t),\ k = 0, 1, \ldots} \qquad \textbf{Eq. 9}$$

Where λ_k is the k-th moment of the radical distribution and μ_k is the k-th moment of the dead polymer distribution. By inserting this definition into the kinetic equations of the polymerization reaction leads to a system of ordinary differential equations.

The infinite sequence of μ_k determines the distribution density D_s, but obtaining the infinite sequence is impossible. The computation of some statistical moments is useful when the objective is to describe properties depending only on a few moments (as an example, properties related to M_N or M_W) or to compare a model to some experimental data. In fact, the number average and the weight average molecular weights can be rewritten as a function of the statistical moments:

$$\boldsymbol{M_N = \frac{\mu_1}{\mu_0} M_M} \qquad \textbf{Eq. 10}$$

$$\boldsymbol{M_W = \frac{\mu_2}{\mu_1} M_M} \qquad \textbf{Eq. 11}$$

Whereas the total polymer chain length distribution is needed, the statistical moment treatment will be unsatisfactory.

2.2.2. Laplace transform based methods

A generating function is a powerful tool for solving problems. It is a formal power series having only one variable, whose coefficients contain information of a sequence of numbers a_n, indexed by natural numbers.

A probability mass function of a discrete random variable X is a function that gives the probability of that variable being equal to some value:

$$f_X(x) = P\{X = x\}$$

It has two basic properties, all the values of the function must be non-negative and their sum must be equal to 1.

A probability generating function is an ordinary generating function which has a_n coefficients equal to the probability mass function of the discrete random variable:

$$G(a_n; x) = \sum_{n=0}^{\infty} a_n x^n$$

Jackson; Small and Whiteley (1973) presented a method that used generating functions to calculate the moments of the MWD of a system that included branching, radical termination by disproportionation and combination and chain transfer to polymer and to a chain transfer agent inside a continuous stirred tank reactor (CSTR). The basic idea was to introduce two sets of generating functions related one to the dead polymer molecules and the other for the radicals. After manipulating this generating function set it was possible to find a differential equation able to determine the polymer moments only using physical properties of the system such as residence time, reaction constants and rate of initiation. In the same paper, the authors derived the same final differential equation by using a Laplace transform which replaced the discrete MWD by a continuous distribution.

Later, Whiteley and Harriga (2001) showed how, in addition to calculating the moments, the generating function could be used to generate a continuous MWD. Recalling the fact that the generating function is the Laplace transform of the MWD, the authors concluded that, in order to obtain a complete MWD, the most direct way was to carry out a numerical inversion of the generating function. Notwithstanding the derivation of the method for numerical inversion of Laplace transforms is not an aim of this thesis, it is

important to present some general aspects in the interest of a better understanding of the strong and weak point of this method.

A 'class of densities' is selected, called $f_{nm}(t;a)$, where a is a positive real number, m a positive integer and n a zero or positive integer. This family of equations presents some interesting properties: imposing $n=m$, it generates a narrow peak shaped function centered at $t=\tau=ln(2)/a$. The integrated area is equal to 1 and the peak narrows as n and m increase.

Figure 2-5 Plots of $f_{nm}(t;a)$ (1); $exp(-t)f_{nm}(t;a)$ (2); $exp(-t)$ (3); $\int_0^\infty exp(-t)f_{nm}(t;a)$ (4); n=m=32; a=ln(2)/0.25

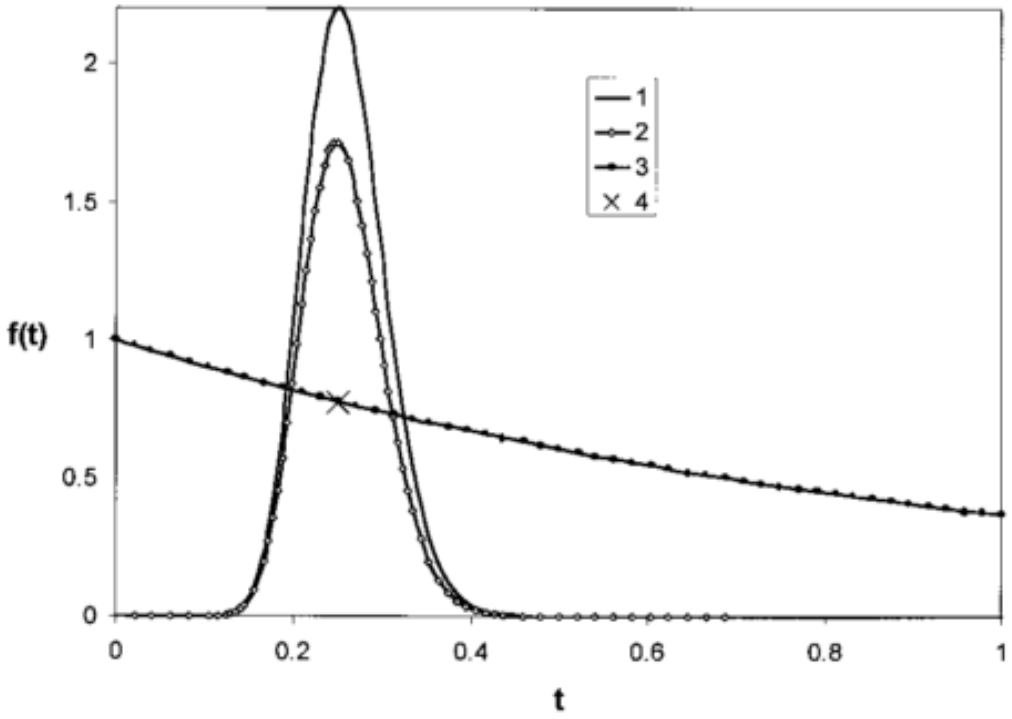

Source: (WHITELEY; GARRIGA, 2001)

As an example of the use of this class of functions it is possible to see how the value of the function $\exp(-t)$ is approximated in $t = 0.25$. One has $\exp(-0.25) = 0.7788$ and $\int_0^\infty \exp(-t)\, f_{nm}(t;a) = 0.7561$ when $n=m=8$. Increasing the value for n and m results in a better approximation at the expense of the computational time, being that these parameters appear as factorials in the function $f_{nm}(t;a)$. So, the authors' idea is to replace the exponential function with an unknown function, expecting a good approximation provided this function changes only slowly in the region of evaluation. By manipulating

the equations the conclusion is that the approximation of the inverse Laplace transform can be calculated as a sum of a series of weighted Laplace transforms.

The strength of this method is the possibility to control the desired precision and the relatively good approximations obtained. The simulation of distributions with a low polydispersity index ($P_D \leq 4$) or with a bimodal trend (as showed in Figure 2-6) can be problematic and not accurate.

Figure 2-6 Example of a bimodal MWD

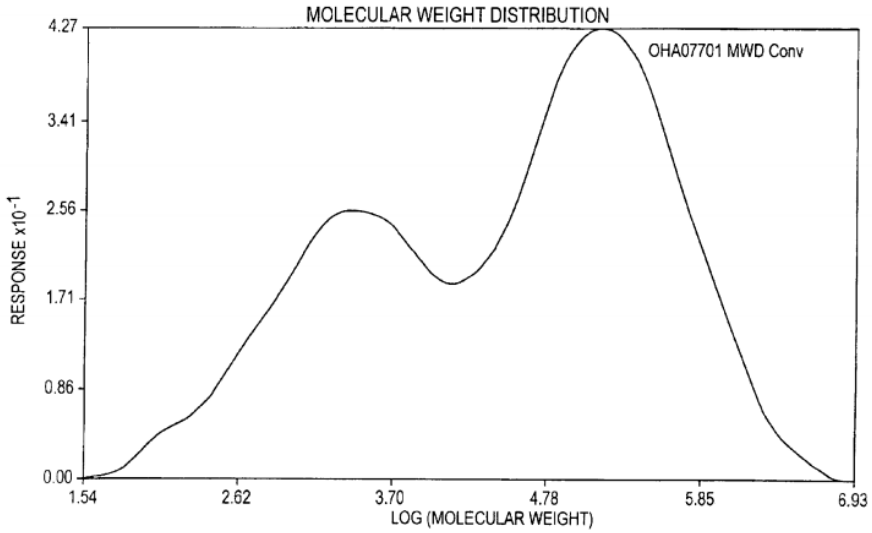

Source: (HAMED; MOMAN; ABU-RAQABAH, 2004)

2.2.3. Interval splitting method

This method was introduced by Crowley and Choi (1998) with the aim of controlling the evolution of the MWD in a batch reactor in order to stop the reactor operation when the polymer tensile strength - directly related to the MWD - reached a desired value, thus optimizing the reaction time.

The idea behind this method is to introduce a function *f(m,n)* which expresses the weight fraction of the polymer that belongs to the interval *(m,n)*:

$$f(m,n) = \frac{\sum_{i=m}^{n} iD_iV}{\sum_{i=2}^{\infty} iD_iV}$$

Depending on the kinetic mechanism of the reaction it is possible to derive the function f(m,n) and process the equation in different ways. For example, considering the solution

polymerization of methyl methacrylate (MMA), it is possible to neglect the termination by combination and the derivate of the function becomes:

$$\frac{df(m,n)}{dt} = \frac{k_p MV}{\lambda_1}\left(\left[\frac{m(1-\alpha)+\alpha}{\alpha}\right]\alpha^{m-1} - \left[\frac{(n+1)(1-\alpha)+\alpha}{\alpha}\right]\alpha^{n}\right)P - \frac{f(m,n)}{\lambda_1}\frac{d\lambda_1}{dt}$$

Where α is the probability of propagation defined as:

$$\alpha = \frac{k_p M}{k_p M + k_{fm} M + k_{fs} S + k_{td} P}$$

The user has the total control of the desired chain length intervals "i" that have to be calculated and, fixing this number n and m can be defined as:

$$m = 2 + a(i-1)i$$
$$n = 1 + a(i+1)i$$

Finally, here "a" is a parameter (positive integer) useful in order to introduce a stopping criteria defined as it follows:

$$f(2,1+ai(i+1))|_{x_c = x_{cf}} \geq 0.999$$

In this way, "a" is selected so that the total weight polymer fraction computed is at least 99.9% of the total polymer produced at the final monomer conversion.
This method provides a fast solution to calculate the shape of the MWD and here are some simulations made with this model.

Figure 2-7 MWD of MMA (only termination by disproportionation), i=40, a=4, simulation time 2.8 s on a Intel Core 2 Duo 2.4 GHz

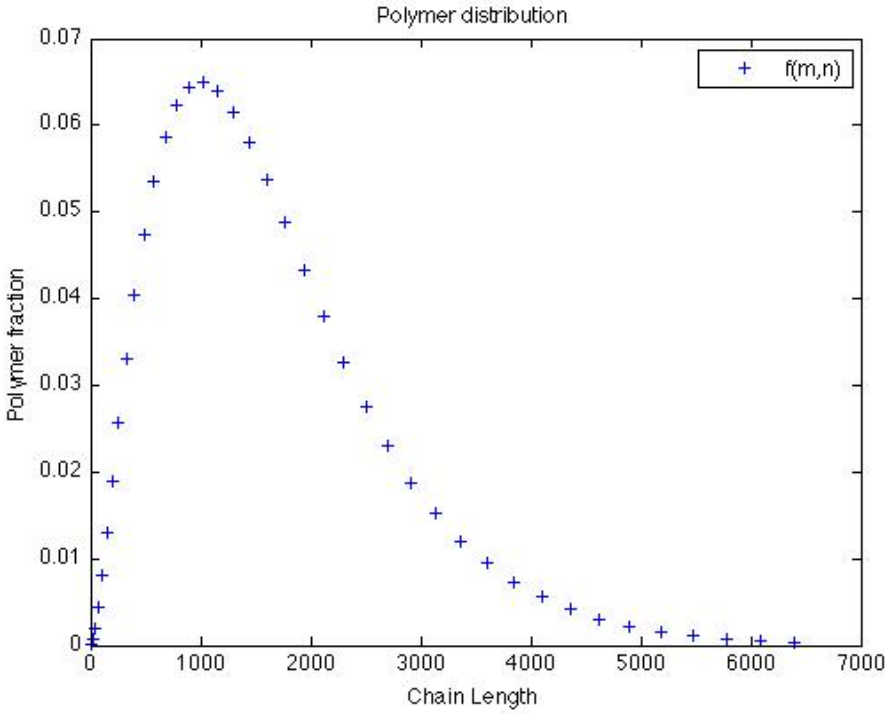

Source: (MELLONI, 2014)

Figure 2-8 MWD of polystyrene (only termination by combination), i=35, a=2, simulation time 59 s on a Intel Core 2 Duo 2.4 GHz

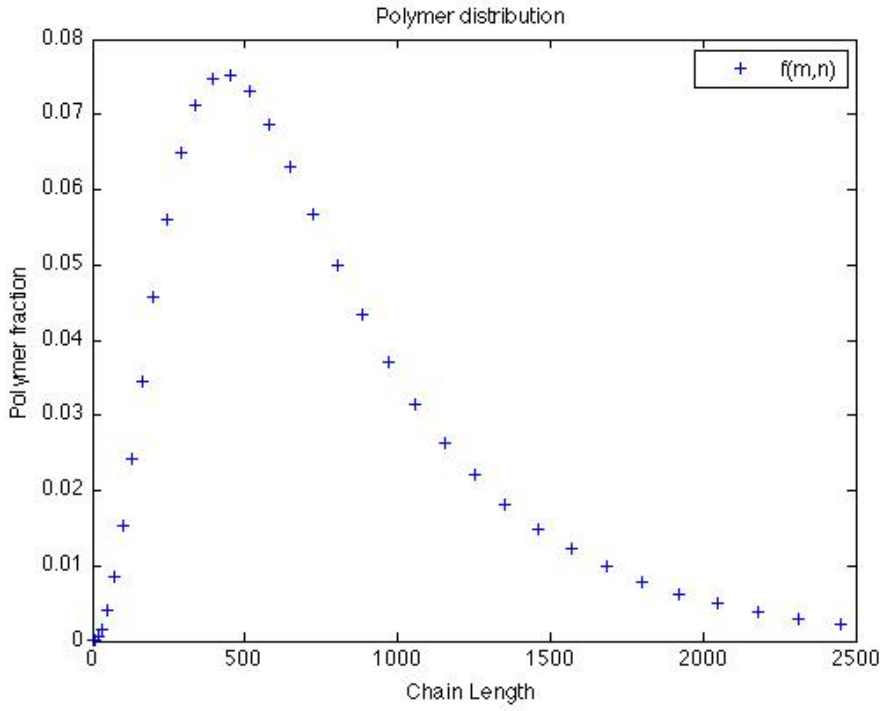

Source: (MELLONI, 2014)

The principal advantages of this method are the speed with which it is possible to compute the MWD in the reactor's conditions and the possibility to decide how many intervals have to be used in the computation. However, it is important to emphasize the fact that this is not a complete MWD and, in order to have a continuous distribution, an interpolation process must be accomplished carrying errors and uncertainties. Moreover, the authors of the work do not study the behavior of this method facing distributions with bimodal trends and do not have the possibility to implement complications such as the termination rate constant k_{tc} and k_{td} depending on the chain length of the involved macromolecule.

2.2.4. Discrete Galerkin method

This technique was introduced by Deuflhard and Wulkow (1989) and used in various other works such as Budde and Wulkow (1991). It consists of a combination between the statistical moment treatment and the Galerkin method. Galerkin methods are a class of methods that convert a continuous operator problem such as a differential equation in time or in space to a discrete problem.

It is characterized by a Galerkin approximation on the basis of orthogonal polynomials that are written in terms of a discrete variable which, in this case, is the degree of polymerization. The objective is to describe the MWD as a finite sum of orthogonal polynomials, calculating their coefficients from the polymerization kinetic scheme. Basically, the MWD $P_S(t)$ can be expanded into certain orthogonal polynomials l_k that are constructed by means of a weighting function ψ:

$$P_S(t) = \psi(s;\rho)\sum_{k=0}^{\infty} a_k(t) l_k(s;\rho)$$

where k is the polynomials degree, a_k are the polynomials coefficients, s is the chain length discrete variable and ρ is an additional parameter.

The Galerkin approximation was developed by truncating the previous infinite series to an index m, generally lower than 20 according to the authors. In order to get a good approximation for small values of m the choice of the weight function ψ becomes crucial,

this is why this function is set to be time-dependent (moving weight function). For MWD related to polymerization processes ψ can be chosen as the Schulz-Flory distribution:

$$\psi\big(s;\rho(t)\big) = (1-\rho(t))\rho(t)^{s-1}$$

The polynomials coefficients are called generalized moments and are computed by means of some differential equations, derived by the use of analytical relations of the orthogonal polymers $l_k(s;\ \rho)$. The user must choose between a large set of orthogonal polynomials that can be used to expand the MWD. In this method, *Laguerre polynomials* are chosen, having the characteristic of being orthogonal to the weight function $\exp(-x)$ over the interval [0,+∞]:

$$\int_0^{\infty} \exp(-x)\, l_m(x)\, l_n(x) dx = \gamma_n \delta_{nm}$$

where δ_{nm} is the Kronecker symbol. The *Laguerre polynomials* turned to be orthogonal to the Schultz-Flory distribution weight function and imposing similarities between the MWD $P_S(t)$ and the moving weight function $\psi(s;\rho(t))$ we finally link the generalized moments to the statistical distribution moments giving restrictions for the choice of the parameter ρ:

$$a_0(t) = \mu_0(t)$$
$$a_1(t;\rho) = 0$$

A data pre-processing requiring Laguerre polynomials properties is needed in order to obtain the whole set of ordinary differential equations which solved will give the MWD.
An advantage of this method is the possibility to express and estimate the relative truncation error in order to describe the quality of the approximation. The authors simulated various MWDs for different values of the truncation index and the error was 6% for a truncation index of 2 and 0.00017% for a truncation index of 15. Moreover, the quasi steady-state assumption (QSSA) for the radical species appeared to have significant deviations from the rigorous computation of the MWD only before reaching

the stationary state in the reactor; after passing the stationary state required time the rigorous computation and the QSSA computation gave the same results.

Another advantage of this method is that a continue MWD is obtained, generated from the generalized moments connected with the statistical moments, thus considering the kinetic polymerization scheme.

A clear disadvantage of this method is the usage of a weight function. The method is not flexible and, in order to turn the method more general and applicable to other distributions, the authors extended the dependence of the weight function to a third additional parameter: $\psi(s;\rho,\alpha)$. Varying the value of α it is possible to describe distributions such as the Schulz-Flory distribution and the Poisson distribution but the method is still restricted to distributions of a certain form.

2.3. About the direct integration

Actually, with the development of more powerful computers, it is possible to compute a direct numerical integration of the equations representing the full MWD. Saldìvar-Guerra et al. (2010) published a work with an eloquent name: "Returning to Basics". The principal idea of the authors is the same of this work with the exception that, in the published work, a quasi-steady-state assumption (QSSA) is made with respect to the radical species. In fact, the ODE system involved in the direct integration presents some typical characteristics like stiffness, which will be discussed later (see section 3.1). The authors state that such a system can be integrated in two different ways: without making the QSSA or making the QSSA on the radical species. In the first case, an implicit integration method is required. In the second case, the ODE system becomes a differential-algebraic system (DAE) whose resolution can be challenging. The authors' purpose is to solve the problem with the second method (making the QSSA) and split the problem into two parts: an algebraic part composed by radicals and a differential part composed by all the other species. Finally, specific numerical methods are applied to solve the two parts. The principal motivation given by the authors that relies behind such a decision is that the implicit methods require the resolution, after one or several time steps, of a full Jacobian matrix with a typical dimension of N_{max}^2 [1]or greater.

[1] N_{max} is a parameter representing the maximum length reached by the radicals in the system. Further explanations are given in section 3.1.

Chapter 3. Rigorous Computation of the Molecular Weight Distribution for a Styrene Polymerization

As it has been seen in the previous chapter, there are different methods to compute a molecular weight distribution and, at the same time, to avoid the computation of the whole set of ordinary differential equations related to the polymerization kinetics. Nonetheless, it can be seen that every type of method presents both advantages and disadvantages. Basically, one may summarize the advantages in terms of computational time required to compute the whole MWD (or at least some points), while the main disadvantages are, in some cases, a leak of information and, in other cases, a long data pre-processing and the introduction of several hypothesis such as the distribution shape (in the form of a weight function). The rigorous computation minimizes the assumptions related to the kinetic system and/or to the MWD shape and solves the entire number of ODEs. In this chapter, the rigorous computation method will be presented and discussed in terms of results, computational time requirements and comparisons with experimental distributions.

3.1. Setting up the system

Recalling the kinetics of a free radical polymerization system one has:

- Initiation

$$I \xrightarrow{k_d} 2R$$

$$R + M \xrightarrow{k_i} P_1$$

- Propagation

$$P_i + M \xrightarrow{k_p} P_{i+1}$$

- Chain Transfer

$$P_i + S \xrightarrow{k_{fs}} D_i + S^*$$

$$S^* + M \xrightarrow{k_{fs}} S + P_1$$

$$P_i + M \xrightarrow{k_{fm}} D_i + P_1$$

- Termination

$$P_i + P_k \xrightarrow{k_{tc}} D_{i+k}$$

$$P_i + P_k \xrightarrow{k_{td}} D_i + D_k$$

3.1.1. Free radical polymerization balance equations

From this kinetic scheme it is possible to write the balance equation for every species involved in the reaction:

- Initiator

$$\frac{dI}{dt} = -k_d I \qquad \textbf{Eq. 12}$$

- Initiator's radical

$$\frac{dR^*}{dt} = 2fk_d I - k_i R^* M \qquad \textbf{Eq. 13}$$

- Monomer

$$\frac{dM}{dt} = -k_i R^* M - k_p M \sum_{i=1}^{\infty} P_i^* + k_{fs} S P_1^* - k_{fm} M \sum_{i=2}^{\infty} P_i^* \qquad \textbf{Eq. 14}$$

- Monomer's radical

$$\frac{dP_1^*}{dt} = k_i R^* M - k_p P_1^* M - k_{tc} P_1^* \sum_{i=1}^{\infty} P_i^* + \left(k_{fs} S + k_{fm} M\right) \sum_{i=2}^{\infty} P_i^* \qquad \textbf{Eq. 15}$$

- Polymer's radical

$$\frac{dP_n^*}{dt} = k_p P_{n-1}^* M - k_p P_n^* M - k_{tc} P_n^* \sum_{i=1}^{\infty} P_i^* - \left(k_{fs} S + k_{fm} M\right) P_n^* \qquad n \geq 2 \qquad \textbf{Eq. 16}$$

- Dead polymer

$$\frac{dD_n}{dt} = \frac{1}{2} k_{tc} \sum_{i=1}^{\infty} P_i^* P_{n-i}^* + \left(k_{fs} S + k_{fm} M\right) P_n^* \qquad \textbf{Eq. 17}$$

when combining two polymer radicals having length $\frac{n}{2}$ there is not the $\frac{1}{2}$ factor

- Solvent

$$\frac{dS}{dt} = -k_{fs} S \sum_{i=i}^{\infty} P_i^* \qquad \textbf{Eq. 18}$$

In these equations, some assumptions are made. The styrene terminates predominantly via combination mechanism (SALDIVAR-GUERRA; VIVALDO-LIMA, 2013) and the disproportionation mechanism is negligible. Moreover, this fact is stood out in some studies where the influence of the disproportionation mechanism has been studied: the

higher the temperature, the lower the disproportionation contribution is, passing from a 20% contribution at 50°C (BERGER; MEYERHOFF, 1975) to a 5.4% contribution at 90°C (ZAMMIT et al., 1997). The volume variation of the system is neglected and there is no dependence of the kinetic constants with the molecule chain length (especially for the propagation and termination kinetic constants).

Moreover, when certain species have a very short time of existence with respect to other species, it is possible to apply the quasi-steady-state approximation (QSSA). This is the case of radical species in the polymerization system; it is very common to apply the QSSA to the initiator's radical species:

$$\frac{dR^*}{dt} = 2fk_dI - k_iR^*M = 0 \qquad \textbf{Eq. 19}$$

And consequently:

$$2fk_dI = k_iR^*M \qquad \textbf{Eq. 20}$$

Obviously, it is impossible for the computer to solve an infinite number of ODEs. It will thus be necessary to define a maximum chain length of the system (N_{max}) in order to reduce the infinite set of ODEs to a finite system of equations. Such an approach has already been used by Chaimberg and Cohen (1990). The problem deriving from this method is that an arbitrary truncation for the maximum chain length reached by the system does not guarantee that we are being consistent with the reality: the real system may reach chain lengths larger than the highest chain length imposed to the computer. To solve this problem, the statistical moment treatment has been coupled to the rigorous computation method as it follows: a first simulation of the zero moment is made in order to obtain the numerical value of $\mu_0 = \sum_{s=1}^{\infty} D_s$ which is the total concentration of the dead polymer in the system. After this, the rigorous truncated ODE system is solved and the total concentration C_{TOT} of the dead polymer obtained is compared to μ_0. If $C_{TOT} < \mu_0$ the maximum chain length truncation of the rigorous system should be augmented, otherwise the quantity of dead polymer that is not being computed by the rigorous system is negligible.

Let us define the number of the equations of the polystyrene system; N_{max} is the maximum length reachable by a radical macromolecule:

- one equation for the initiator
- No equation for the initiator's radical (QSSA)

- one equation for the monomer
- one equation for the solvent
- (N_{max}) equations for the polymer's radical
- ($2N_{max}$-1) equations for the dead polymers (starting from 2 monomeric attached units, D_2)

$$2N_{max} - 1 + N_{max} + 1 + 1 + 1 = 3N_{max} + 2$$

The ordinary differential equations to be solved are $3N_{max}$+2 and this will compute a distribution having dead macromolecules ranging from 2 to $2N_{max}$, where $D_{2_{Nmax}}$ is polymer resulting from the combination of the two radicals P^*_{Nmax}.
By considering the molecular weight of styrene (PM_S=104.15 g/mol), in order to compute a distribution covering molecular weights up to 210,000 g/mol it will be necessary to fix N_{max}=1000, thus solving 3002 ODEs.

3.1.2. Numerical methods used for the direct integration of the ODE system

The numerical computing environment MATLAB has been used to solve this system. The software provides some tools intended as functions that are specifically oriented to ODEs systems. The choice of the function used to solve the system is crucial and needs to satisfy criteria such as solution accuracy and computational time requirements. Having some experience with chemical kinetics helps in the choice of the correct function: in general, systems that lead with radical species are, in computational terms, stiff (FERNANDO, 2013).
Stiffness is typical in a system that involves "quick" dynamic changes combined with "slow" dynamic changes. In facts, the production and consumption rate of a radical species is orders of magnitude greater than the one of a dead polymer. Consequently, for a small time-step (or length-step, depending on what kind of reactor is used) size taken in the numerical method used to solve the system, some equations may vary much more than others and this is the origin of numerical issues.
Rigorously, there is not a universally accepted definition of stiffness. Some authors examine the behavior of fixed step size solutions, other introduce indexes, such as stiffness index, related to the eigenvalues of the Jacobian matrix. (SPIJKER, 1996) states

that "stiffness occurs if the largest step size guaranteeing numerical stability is much smaller than the largest step for which the local discretization error is sufficiently small". Consequently, when solving the differential equations, there are components which vary much more rapidly than others (this is the case for the radical species). This criterion is formalized by the requirements

$$\frac{max|Re\ \lambda|}{min|Re\ \lambda|} \gg 1$$

assuming that the eigenvalues λ of the Jacobian matrix are all negatives[2].

Typically, a system is considered to be stiff if the latter ratio is greater than 10^4 (FERNANDO, 2013).

MATLAB provides various functions designed to solve stiff problems: *ode15s*, *ode23s* and *ode23tb*:

- ode15s is based on the numerical differentiation formulas (NDFs[3]). It can optionally use the less efficient backward differentiation formulas (BDFs[4])
- ode23s is based on a modified Rosenbrock formula of order 2.
- ode23tb is an implicit Runge-Kutta formula with a first stage that is a trapezoidal rule step and a second stage that is a BDF of order 2.

3.2. Computation time requirements

First, in order to analyze the performance of the rigorous resolution method, the computation time for solving the ODE system is analyzed. The reaction is the polymerization of styrene and reaction conditions are presented in Table 1.

[2] The Jacobian matrix is strictly related to the concept of stability. The Poincare-Lyapunov theorem links the stability to the eigenvalues of the Jacobian matrix: if they are negative or complex with a negative real part the associated point is a sink and the solutions will spiral around the equilibrium point. Otherwise, if they are positives or complex with positive real part, the associated point is a source and the solutions will move away (MASSOUD).

[3] See section 6.3.2 for a brief explanation.

[4] See section 6.3.1 for a brief description.

T [K]	P [atm]	Time [min]	M_0 [mol/L]	I_0 [mol/L]	S_0 [mol/L]
373.15	1	80	4.8824	$6.8794*10^{-3}$	3.5233

Table 1 Reactor's condition for the computation of the time requirements

The kinetic constants used for this simulation are taken from Cutter and Drexler (1982), Hui and Hamielec (1972), Brandrup and Immergut (1989) and are listed in Table 2. These constants were used together by Cabral et al. (2004).

Dissociation constant	k_d *[1/min]*	$1.0272 * 10^{17} exp\left(\frac{-15924}{T}\right)$
Propagation constant	k_p *[L/mol/min]*	$6.306 * 10^{8} exp\left(\frac{-3577}{T}\right)$
Termination constant	k_{tc0} *[L/mol/min]*	$7.53 * 10^{10} exp\left(\frac{-844}{T}\right)$
Monomer chain transfer constant	k_{fm} *[L/mol/min]*	$1.2 * k_p * 10^{-5}$
Solvent chain transfer constant	k_{fs} *[L/mol/min]*	$7 * k_p * 10^{-5}$

Table 2 Kinetic constants for the computation of the time requirements

Notice that the termination rate constant is called k_{tc0} because of the gel effect that changes its value during the reaction.

In this simulation, the interest is not representing the whole MWD but rather to understand how the computation time is related to the parameter N_{max}. The zero-moment is not calculated, because there is no need to compare the results of this simulation with other data, since it is obvious that the fact that the results for low values of N_{max} do not represent a physical reality.

The ODE system has been solved in a computer with an Intel Xeon E5645 2.40 GHz processor and the results of the computation are shown in Figure 3-1.

Figure 3-1 Computational time plot versus the parameter N_{max} with data regression.

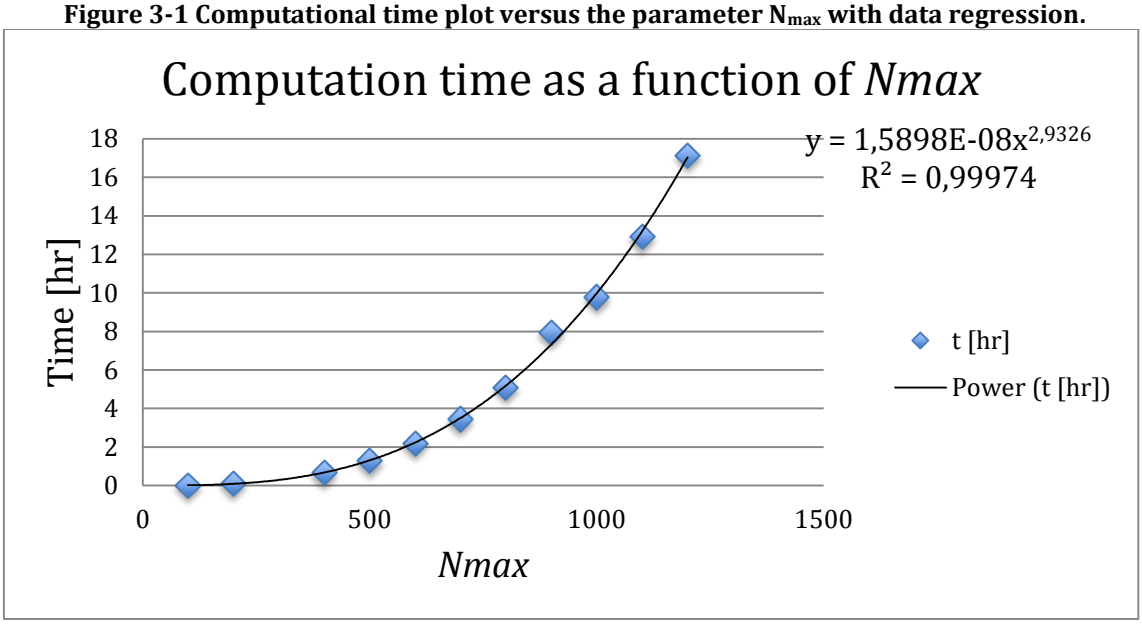

Source: (MELLONI, 2014)

As it is possible to see, the computation time obviously increases with the increase of N_{max}. Unfortunately, its trend follows a power function and, in this specific case, it is $t(N_{max}) = 1.5898 * 10^{-8} * N_{max}^{2.9326}$. This means that for a small increase of N_{max}, that is, a small increase of the maximum molecular weight computed, a much longer time will be required in order to complete the simulation.

3.3. Choosing N_{max} - Stopping Criteria -

In this section the choice of N_{max} is discussed. As anticipated previously in section 3.1, the choice of Nmax is based on the resolution of the ordinary differential equations derived from the statistical moment treatment. It will now be given an example of this procedure based on a polystyrene polymerization with initiation, propagation, chain transfer to monomer and solvent and termination by combination. The equations derived from the statistical moment treatment are:

$$\frac{dI}{dt} = -k_d I \qquad \text{Eq. 21}$$

$$\frac{dM}{dt} = -k_p M \lambda_0 - 2 f k_d I - k_{fm} M \lambda_0 \qquad \text{Eq. 22}$$

$$\frac{d\lambda_0}{dt} = 2 f k_d I - k_{tc} \lambda_0^2 \qquad \text{Eq. 23}$$

$$\frac{d\mu_0}{dt} = k_{fm} M \lambda_0 + k_{fs} S \lambda_0 + \frac{k_{tc}}{2} \lambda_0^2 \qquad \text{Eq. 24}$$

$$\frac{dS}{dt} = -k_{fs} S \lambda_0 \qquad \textbf{Eq. 25}$$

It can be seen that only 5 equations need to be solved in order to compute some properties of the distribution. The reaction conditions are the same as listed in Table 1 and the kinetic constants used are those shown in Table 2. Moreover, the initial value for the zero moment of both radicals and polymers is 0. The computation of the entire system requires an average time of 0.52 seconds, which is extremely faster if compared to the rigorous computation. The result of the system is:

$$\mu_0 = \sum_{s=1}^{\infty} D_s = 0.0046 \left[\frac{mol}{L}\right]$$

The rigorous computation is then applied for various values of N_{max} and the plot of the zero moment - calculated by summing all the dead polymers - is compared with the value obtained from the statistical moment treatment. The comparison is shown in Figure 3-2.

Figure 3-2 Comparison between the dead polymer zero moment from the statistical moment treatment and that from rigorous computation

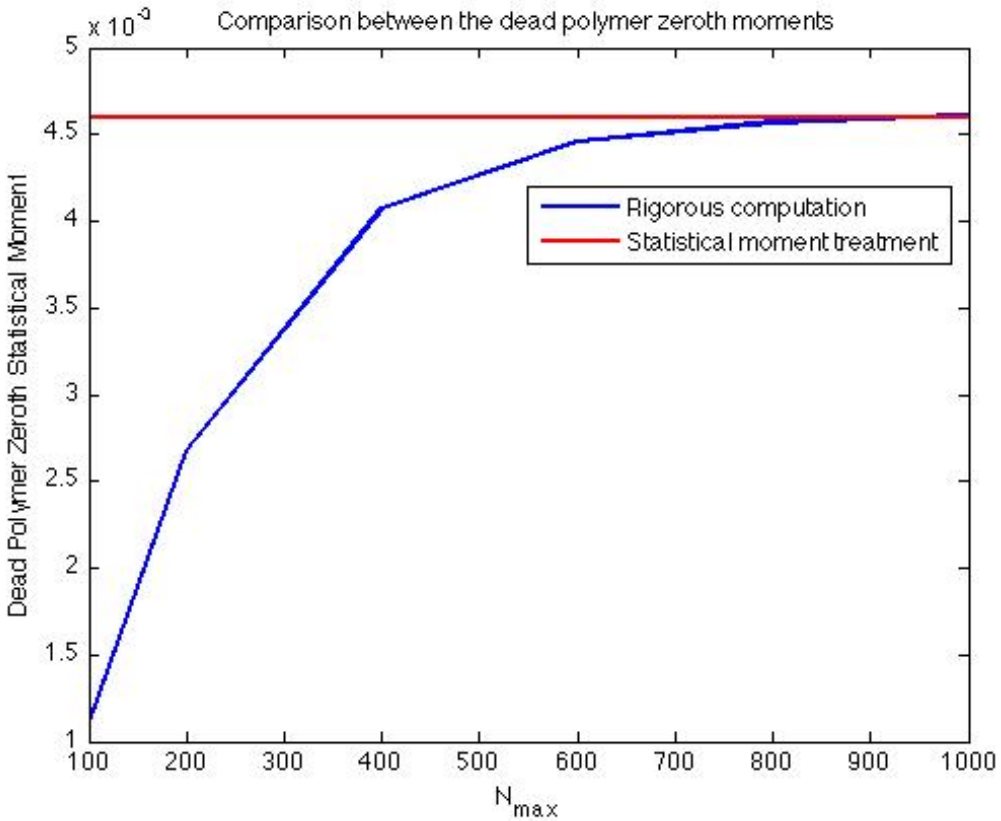

Source: (MELLONI, 2014)

Figure 3-2 shows that, as N_{max} increases, the dead polymer zero moment tends to an asymptotic value. When this value is reached, the system is considered to be complete (i.e. the maximum polymer length, $2N_{max}$-1, includes all the macromolecules produced and those excluded -macromolecules longer than $2N_{max}$-1- are a negligible quantity).

3.4. Termination rate constant

The termination rate constant has been the object of several studies that tried to describe its behavior as a function of many variables of the system. It is now well established that the termination rate depends on the temperature of the system, chain mobility, length of the diffusing species and composition of the medium (principally, bulk or solution polymerization) (CHIU; CARRATT; SOONG, 1983). If this is true, the termination step should be diffusion-controlled (BARNER-KOWOLLIK; RUSSELL, 2009). In fact, there are experimental evidences to confirm this theory:

- First, during experiments involving radical polymerization, the viscosity of the system was varied and its effects over the overall reaction were determined. It appeared that, besides the reduction of the radical efficiency with the increase of the viscosity, the rate of chain termination showed a behavior inversely proportional to the viscosity: $\bar{k}_t \sim \frac{1}{\eta}$ (FISCHER; MÜCKE; SCHULZ, 1969). This is exactly what one would expect from a diffusion-controlled reaction.
- Second, studies showed how the termination constant decreased as long as the pressure increased (BUBACK; KUCHTA, 1997). This is the same effect that the pressure has over the diffusional coefficient, when considering molecular diffusion[5].

If in the past the question was if there was chain length dependence for the termination constant, actually the question is how this chain length dependence is expressed.

Chiu; Carratt and Soong (1983) proposed that the termination reaction occurs only when two polymer radicals are located within one molecular diameter and are properly oriented. They also explained that due to the fact that a molecular radical increases its length because of the propagation step, it is difficult to describe it with a single molecular weight during its all lifetime.

[5] Excluding particular cases such as, for example, Knudsen diffusion in which the pressure has practically no effects.

In literature it is easy to find correlations introducing a critical parameter such as critical volume factor or critical solution viscosity, in order to activate the gel effect in the computation of the reaction. An example of this is given by Smith; Russell and Heuts (2003) that introduced a critical molecular length above which the termination rate starts to decrease in a different way compared to molecules having length below the critical one. The same concept is applied years later by Najafi et al. (2011). This might be effective or ineffective, depending on the case studied, but certainly it hardly represents the physic reality of what is happening in the system. In fact, this introduces a sort of "discontinuity" in the system: the termination rate is constant until a moment when, reached a certain critical parameter, it starts to progressively decrease. A method that gives continuity in the diminution of the termination rate consists into correlating the kinetic constant with the length of the molecules interacting and weight the chain length effect with an adjustable parameter (MAHABADI, 1985).

$$\boldsymbol{k_{tc}(i,j) = \frac{k_{tc0}}{(ij)^{\alpha}}} \qquad \textbf{Eq. 26}$$

Where k_{tc0} is the termination rate constant estimated for the termination of two monomeric radicals -taken from Fu et al. (2007)-, i and j are the chain length of the two interacting molecules and α is the adjustable parameter regulating the diminution of the termination rate. In literature (BARNER-KOWOLLIK; RUSSELL, 2009) it is possible to find estimations for this parameter which has a order of magnitude of about 10^{-1}.
On the same line of the Eq. 26, which can be seen as a geometric mean, other models have been developed:

$$\boldsymbol{k_{tc}(i,j) = \frac{1}{2} k_{tc0}(i^{-\alpha} + j^{-\alpha})} \qquad \textbf{Eq. 27}$$

$$\boldsymbol{k_{tc}(i,j) = k_{tc0}\left(\frac{2ij}{i+j}\right)^{-\alpha}} \qquad \textbf{Eq. 28}$$

Representing respectively a diffusion mean and a harmonic mean.
It has been demonstrated (Figure 3-3) the very little influence of the type of mean over the final MWD (BARNER-KOWOLLIK; RUSSELL, 2009). This does not mean that there is not a correct model for every situation; it just means that the correct model cannot be determined using experimental MWD.

Figure 3-3 Influence of the termination rate constant model over the final MWD: geometric mean, diffusion mean and harmonic mean

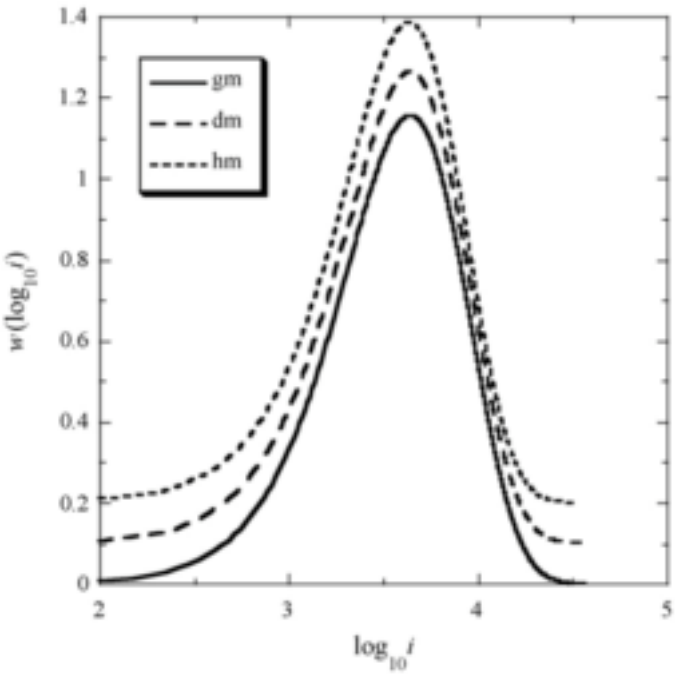

Source: (BARNER-KOWOLLIK; RUSSELL, 2009)

In Figure 3-4 it is possible to see how the termination rate decreases when the interacting molecules become longer, while in Figure 3-5 the effects of α on the kinetic constant for a specific polymeric radical are shown. Finally, in Figure 3-6 there is a plot of the influence of α over the average termination rate constant, calculated as if every radical combination had the same weight.

Figure 3-4 Diminution of the termination rate constant as a function of the length of the interacting radicals

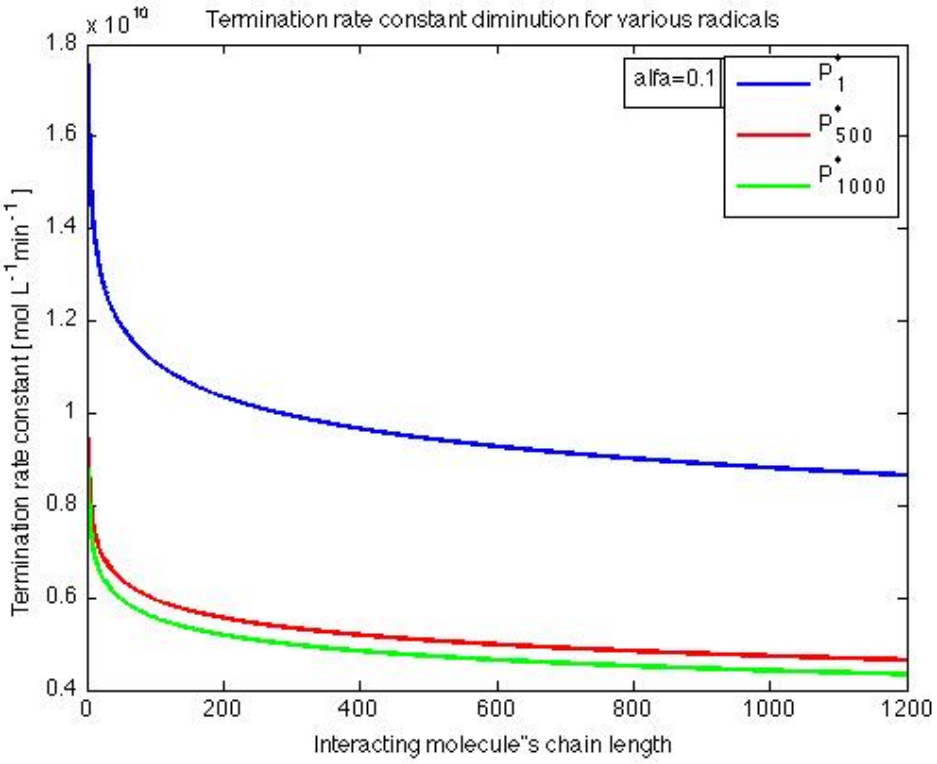

Source: (MELLONI, 2014)

Figure 3-5 Effects of α on the termination rate constant for the radical P^*_{100}

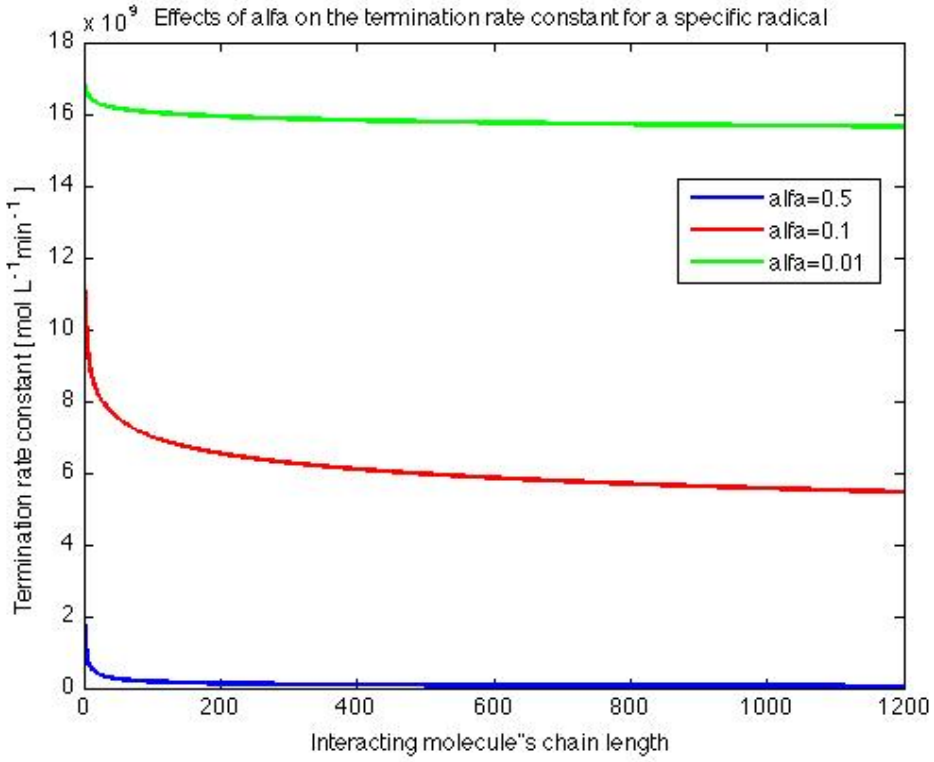

Source: (MELLONI, 2014)

Figure 3-6 Effects of α on the average termination rate constant

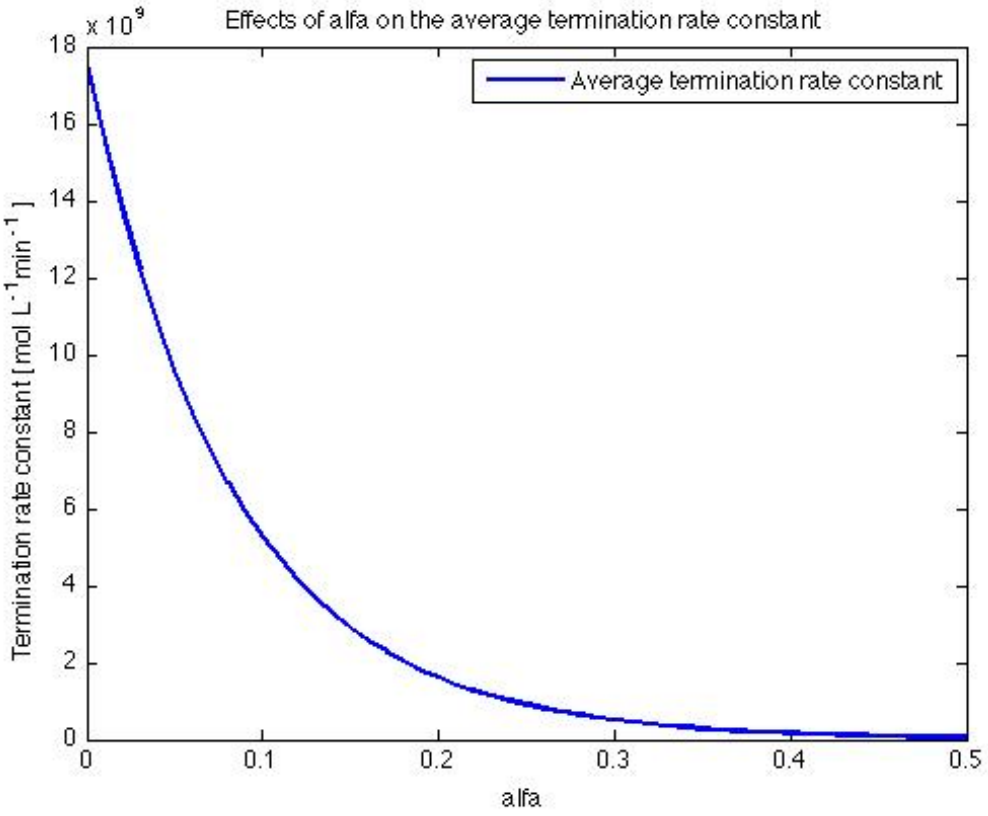

Source: (MELLONI, 2014)

As it is possible to see, the parameter α has a strong influence over the overall termination rate constant, critically reducing the kinetic constant, making the other kinetic steps, specially the propagation step, much more important. It is reasonable to expect wider molecular weight distributions and greater chain lengths as long as α increases, due to the fact that the propagation step becomes dominant with respect to the termination step.

3.4.1. Computational implementation of the termination rate constant

Notwithstanding the fact that the kinetic scheme remains the same, there is an important change, from the mathematical point of view, in the balance equations of the species.

- Monomer's radical

$$\frac{dP_1^*}{dt} = k_i R^* M - k_p P_1^* M - P_1^* \sum_{i=1}^{\infty} k_{tc}(1,i) P_i^* + \left(k_{fs} S + k_{fm} M\right) \sum_{i=2}^{\infty} P_i^* \quad \textbf{Eq. 29}$$

- Polymer's radical

$$\frac{dP_n^*}{dt} = k_p P_{n-1}^* M - k_p P_n^* M - P_n^* \sum_{i=1}^{\infty} k_{tc}(n,i) P_i^* - \left(k_{fs} S + k_{fm} M\right) P_n^* \qquad n \geq 2 \quad \textbf{Eq. 30}$$

- Dead polymer

$$\frac{dD_n}{dt} = \frac{1}{2} \sum_{i=1}^{\infty} k_{tc}(i, n-i) P_i^* P_{n-i}^* + \left(k_{fs} S + k_{fm} M\right) P_n^* \quad \textbf{Eq. 31}$$

when combining two polymer radicals having length $\frac{\mathrm{n}}{2}$ there is not the $\frac{1}{2}$ factor

In practice, the termination by combination constant k_{tc} becomes dependent on the interacting radicals macromolecules and cannot be taken as if it were a constant values for all the species.

Computationally, the following matrix is generated in order to have the entire set of possible combinations:

$$\begin{bmatrix} k_{tc}(1,1) & \cdots & k_{tc}(1, N_{\max}) \\ \vdots & \ddots & \vdots \\ k_{tc}(N_{max}, 1) & \cdots & k_{tc}(N_{max}, N_{max}) \end{bmatrix}$$

3.4.2. Computation time requirements of the new system

The new ODE system was solved for various values of N_{max} in order to determine the performances in terms of computation time. The results are show in Figure 3-7.

Figure 3-7 Computation time plot versus the parameter Nmax with data regression

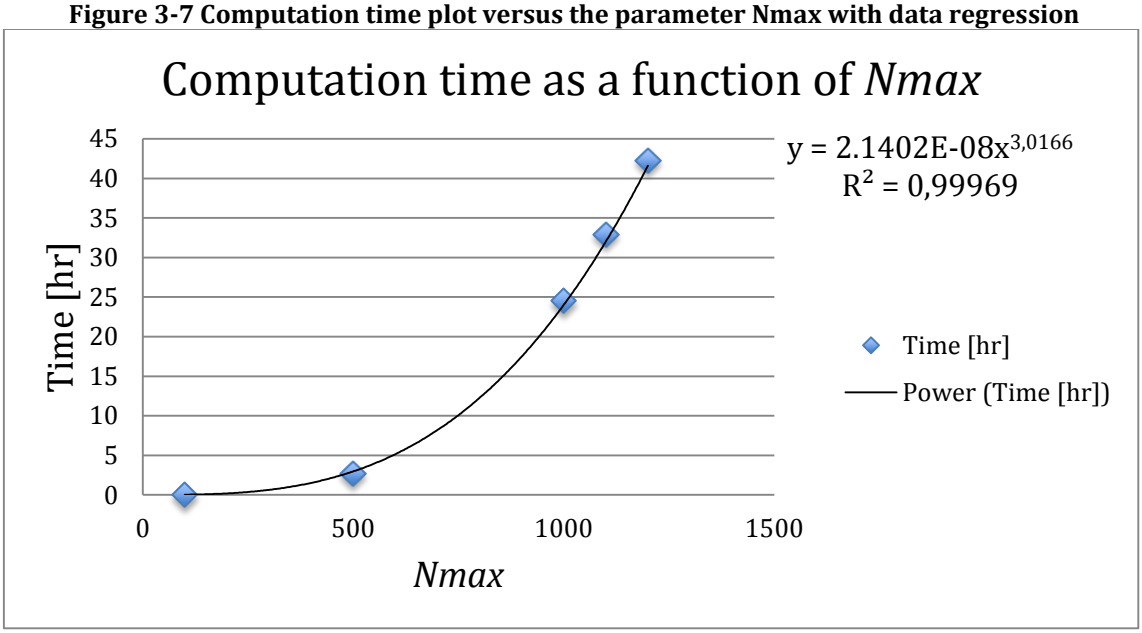

Source: (MELLONI, 2014)

As shown in Figure 3-7, the new system with the variable termination rate needs much more time to compute the entire MWD. An explanation to this might be the fact that a stiff system is very sensible to any change of order of magnitude. In the previous system, the termination rate was constant and maintained its values for every radical or dead polymer species. In this new system, as it can be seen from Figure 3-4, the termination rate for a same species may vary significantly depending on which radical is the interaction with.

3.4.3. Effects of the termination rate constant on the molecular weight distribution

In this section the influence of the coefficient α over the molecular weight distribution is examined. The reaction conditions are shown in Table 3:

T [K]	P [atm]	Time [min]	M_0 [mol/L]	I_0 [mol/L]	S_0 [mol/L]
373.15	1	80	4.8824	$6.8794*10^{-3}$	3.5233

Table 3 Reaction conditions for the evaluation of the influence of α over the MWD.

In Figure 3-8, the effects of α over the molar fraction MWD and the mass fraction MWD are shown. Subsequently, Figure 3-9 shows the effects over the final conversion of the styrene monomer.

Figure 3-8 Mass fraction MWD variation as a function of α

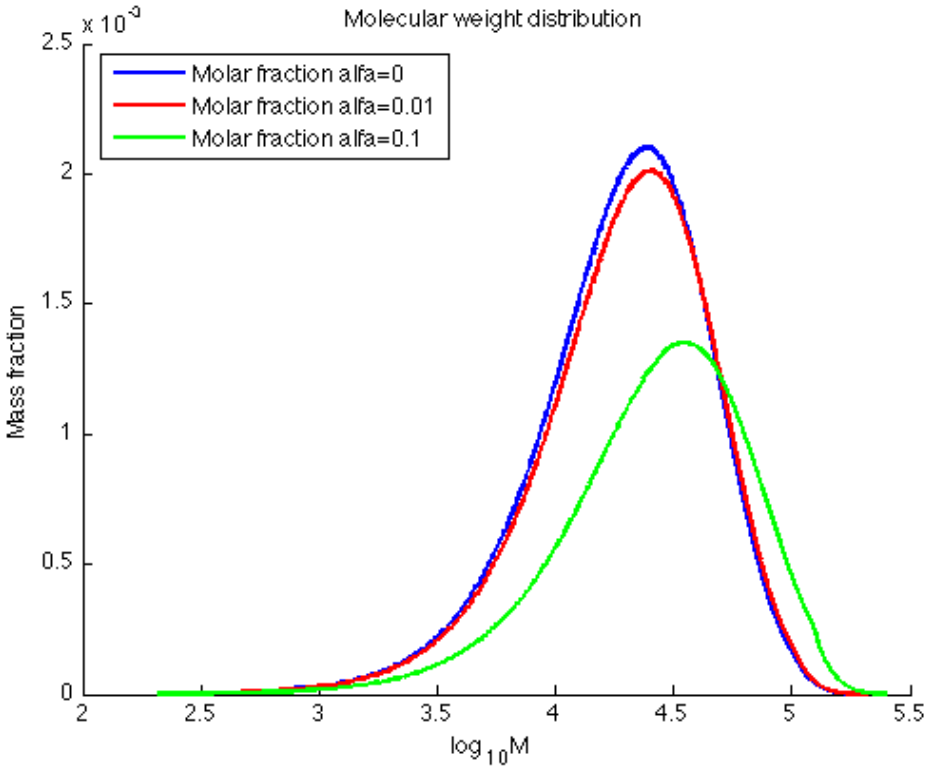

Source: (MELLONI, 2014)

Figure 3-9 Conversion evolution along time as a function of α

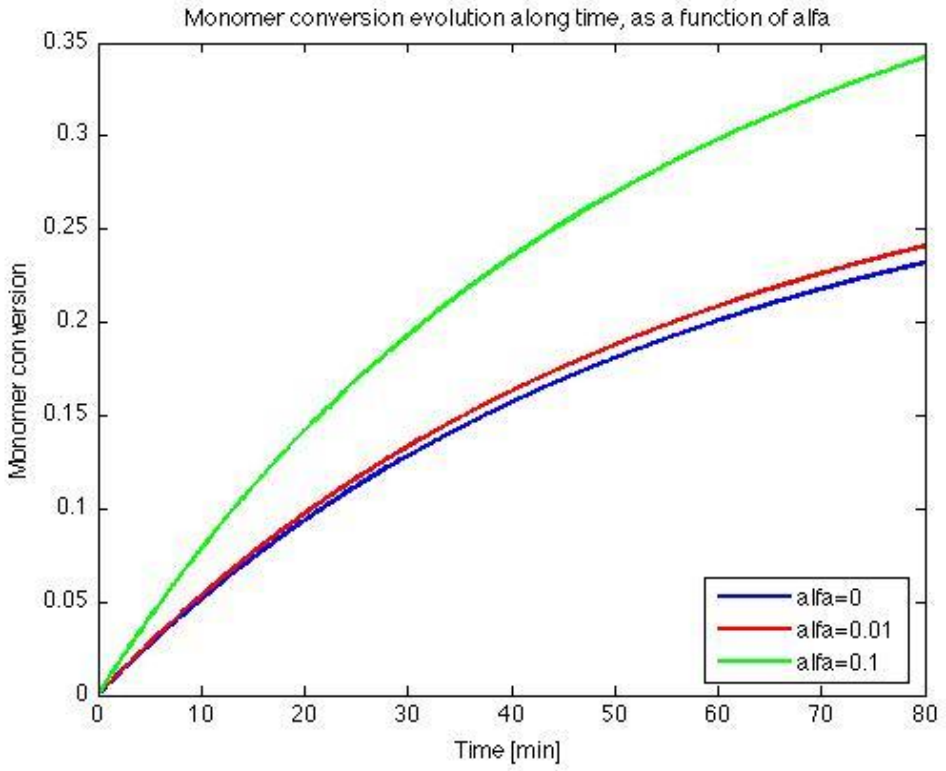

Source: (MELLONI, 2014)

The results are summarized in Table 4 below.

	Monomer conversion	M_N **[g/mol]**	M_W **[g/mol]**	P_D
$\alpha = 0$	0.2321	25,502	40,104	1.57
$\alpha = 0.01$	0.2409	26,405	41,611	1.58
$\alpha = 0.1$	0.3423	36,497	58,903	1.61

Table 4 Comparison between the MWD simulated for several α.

A first hypothesis should be done with respect to the simulation obtained imposing α=0: this system cannot represent a real physical system since all the polymer's radicals have to terminate with the same constant k_{tc0}, which physically represents the termination between two monomeric radicals ($k_{tc0} = k_{tc}(1,1)$). It is possible to affirm that the system with α=0 represents a virtual situation, where the termination step is overestimated, thus underestimating the chain growth during the reaction. This explains why the values for M_N and M_W are so low and the molar and mass fraction MWD are

shifted to the left, having a peak at low molecular weights compared to the distribution derived by imposing α=0.1.

As shown in Figure 3-6, as long as α increases, the termination rate constant decreases, thus promoting the propagation step, making the molecules grow and consequently shifting the molar and mass fraction MWD to the right, with a peak at higher molecular weights values; this effect is enhanced in the mass fraction MWD, shown in Figure 3-8. Moreover, besides having a peak at higher molecular weights, the whole MWD becomes wider with the increase of α.

3.4.4. Comparison between molecular weight distributions computed with constant termination rate and variable termination rate.

For a better representation of the MWD the variation of the termination rate constant should be considered, at the expenses of the computation time. It would be interesting to compare the effects of considering an average termination rate for the whole reaction time and compare the simulation obtained with the MWD obtained considering a different k_{tc} for every species. The comparison is shown in Figure 3-10.

Figure 3-10 Comparison between mass fraction distribution obtained considering variable and average k_{tc}

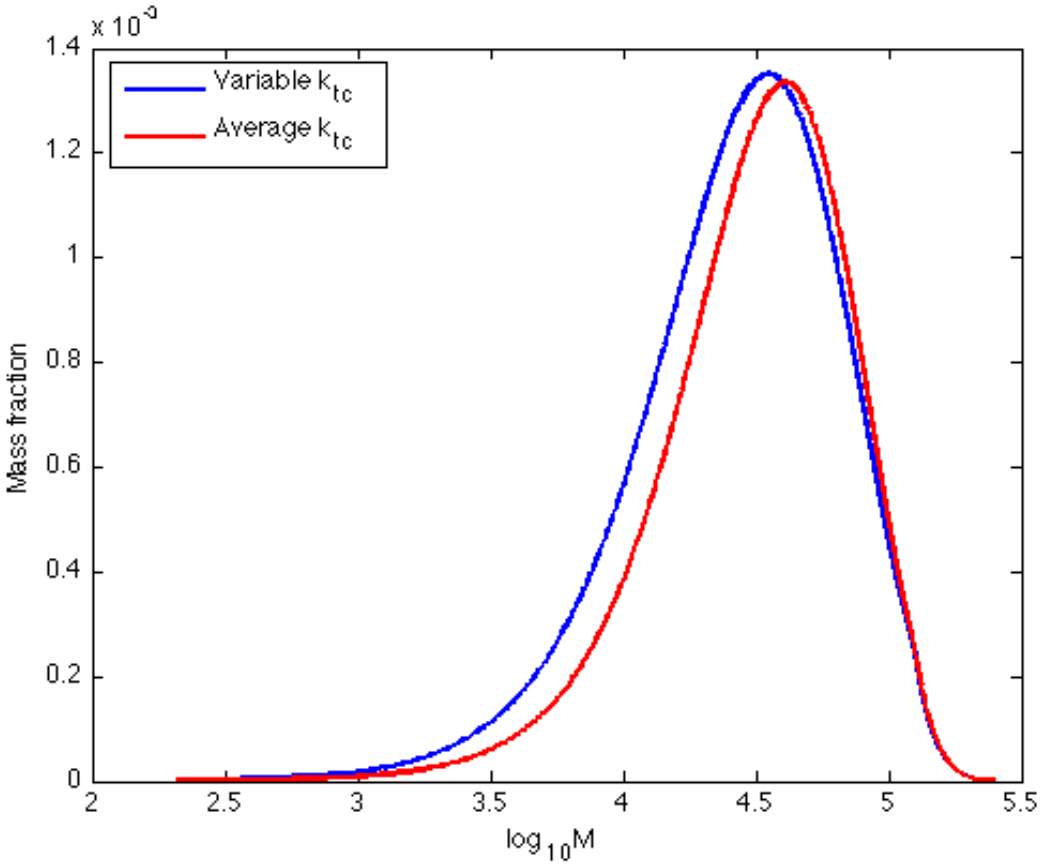

Source: (MELLONI, 2014)

There are differences between the two distributions that can be explained through the way the average k_{tc} was calculated:

$$\overline{k_{tc}} = \frac{\sum_{i=1}^{Nmax}\sum_{j=i}^{Nmax} k_{tc}(i,j)}{N_{max}+\frac{N_{max}^2-N_{max}}{2}} \qquad \textbf{Eq. 32}$$

Where the denominator represents the total number of possible combinations for $k_{tc}(i,j)$, excluding the repetitions with equal indexes. In practice, this is an average in which combination has the same weight. The resulting average termination rate will be underestimated because of the fact that a termination between two relatively small radicals, which is fast, will give the same contribution during the average process than a termination between two long radicals, which is slow; it is obvious that the event of a termination between two small radicals is much more probable than the event of a

termination between two long radicals. Therefore, it will be necessary to introduce a sort of weight to take into account this fact.

One possible solution to reduce the differences between the MWD obtained considering a variable termination rate constant and the one obtained considering an average termination rate constant is to use a weighted variable average. This is done weighting, at every iteration, a new average termination rate constant using the molar fractions of the previous iteration. The results are shown in Figure 3-11 and Table 5.

Figure 3-11 Comparison between molar fraction distributions obtained using variable and average k_{tc}

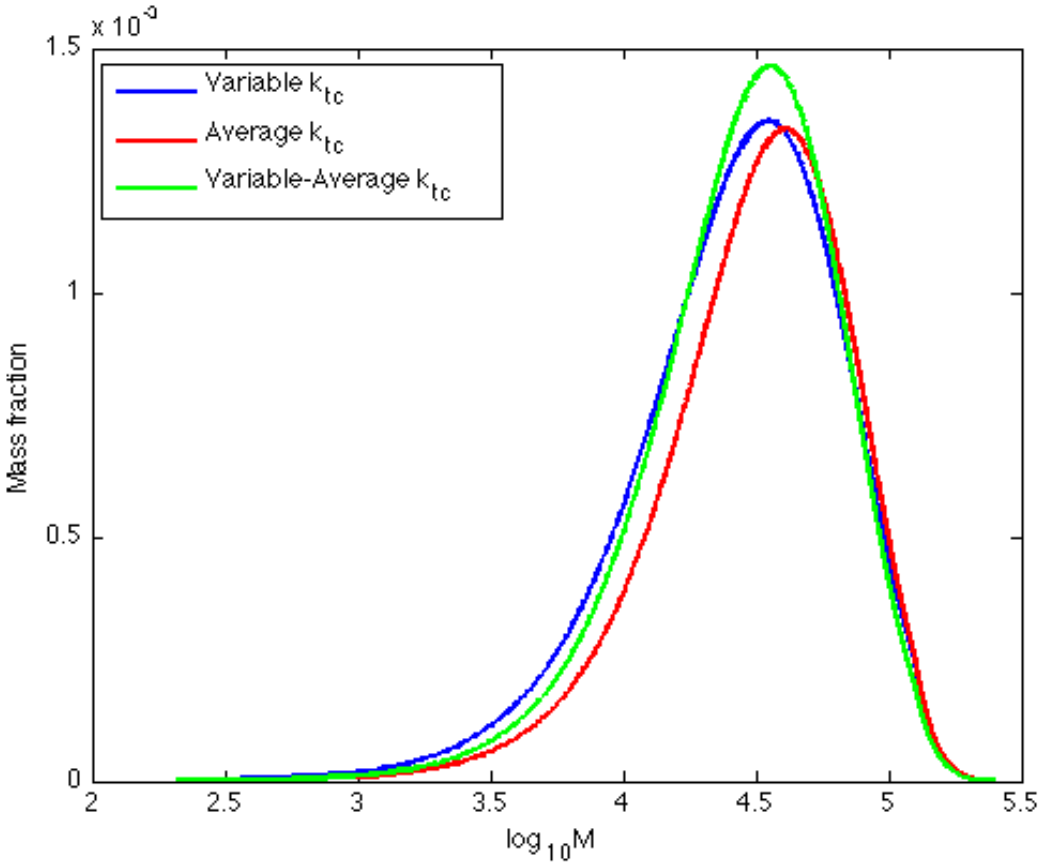

Source: (MELLONI, 2014)

	M_N [g/mol]	M_W [g/mol]	PD	Computational time [hr]
Variable k_{tc}	36,497	58,903	1.61	42.3
Average k_{tc}	40,901	61,715	1.51	22.3
Variable-average k_{tc}	36,844	56,712	1.54	32.1

Table 5 Comparison between M_N, M_W and PD index obtained considering variable and average k_{tc}.

This new method achieves a better representation of the MWD that needs only 75% of the original computation time requirement. The number average molecular weight is well represented while the weight average molecular weight is slightly lower than the original one.

3.5. Towards a higher computational efficiency

In section 3.4.2 it has been shown how, implementing a variable termination rate constant for every interacting pair of radicals, the computational time requirements turned very demanding compared to the system with an invariable termination rate.

The MATLAB function profiler helps to understand how this computational time is distributed along the program, thus helping to identify those code sections that are inefficient.

Besides improving the logical patterns that compose the code, when dealing with stiff systems there is a particular characteristic that turns the solver very slow and inefficient: the Jacobian matrix estimation (SALDÍVAR-GUERRA et al., 2010). The MATLAB help section reports: "For the stiff solvers […] the Jacobian matrix is critical to reliability and efficiency. […] If the Jacobian property is not set, it is approximated by finite differences" (MATHWORKS, 2014).

In fact, providing an analytical Jacobian matrix to the solver allows avoiding a numerical estimation of a matrix having N_{max}^2 elements. In section 6.1 an explanation of how the Jacobian matrix is implemented in the system will be given.

3.5.1. Computational time requirements

As it has been done for the previous systems, an analysis of the computational time requirements of the new system, with the Jacobian, is done. The results are compared to the systems having a constant k_{tc} and a variable k_{tc} but no analytical Jacobian provided.

Figure 3-12 Computation time plot versus the parameter Nmax - Comparison between systems having constant ktc, variable ktc and variable ktc with Jacobian provided

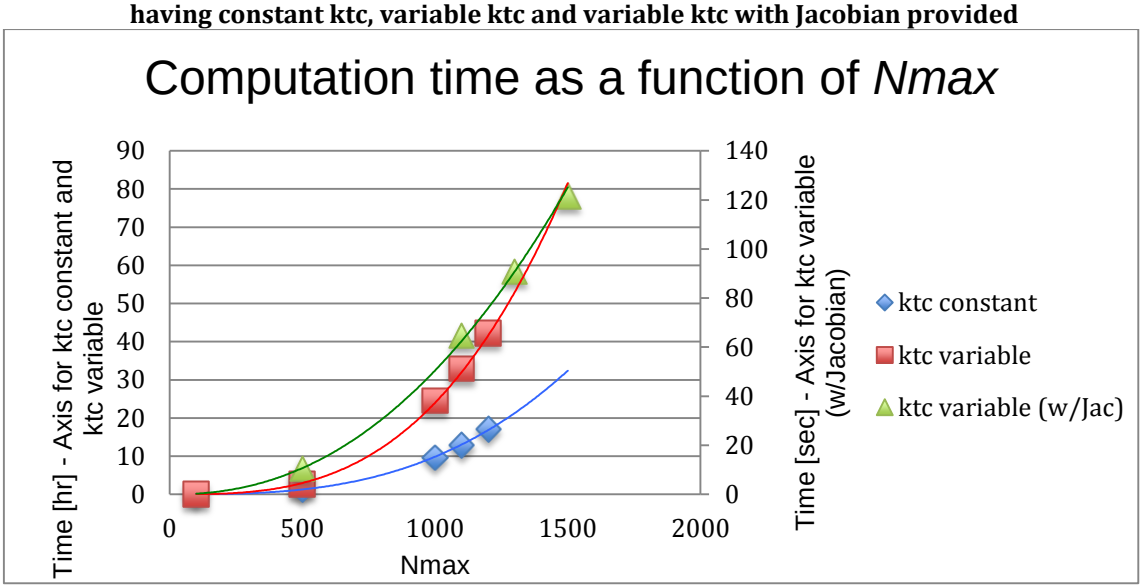

Source: (MELLONI, 2014)

As shown in Figure 3-12 the computational time requirements - when the user supplies the Jacobian - are significantly lower compared to the other systems. For a simulation with N_{max}=1100, the time required to complete the simulation is reduced from 33 hr to 65 s: a reduction of 99.9% of the original computational time.

Recalling the paper published by Saldìvar-Guerra et al. (2010), introduced in section 2.3, it can be said that there is no need to split the system and make the QSSA if the analytical Jacobian matrix is provided.

3.6. Comparison with experimental data – effects of the dilution over α

In this section, some experimental data having different monomer concentrations will be compared to the results predicted by the model. A special focus will be given to the parameter α, which regulates the termination rate constant diminution. In all the cases

presented below, an optimization was made to identify which value of α best represented the experimental data.

3.6.1. Experiments from the literature with different dilutions

3.6.1.1. Monomer 30% wt. (HAMIELEC; HODGINS; TEBBENS, 1967)

The reactor is a conventional batch reactor. The monomer to solvent (benzene) ratio is 30% wt. with 2% wt. of initiator (AIBN). The concentrations related to these conditions are show in Table 6.

T [K]	P [atm]	Time [min]	M_0 [mol/L]	I_0 [mol/L]	S_0 [mol/L]
323.15	1	60	2.4814	0.105	7.5

Table 6 Reaction conditions used by (HAMIELEC; HODGINS; TEBBENS, 1967).

Table 7 and Figure 3-13 show the comparison between the experimental data and the results obtained from the simulation of the experiment. The best approximation was obtained using α=0.08.

α=0.08	***M_N [g/mol]***	***M_W [g/mol]***	**Conversion**
Experimental Result	15,320	23,800	0.03
Simulation Result	14,913	23,631	0.031

Table 7 Comparison between experimental results and model results.

Figure 3-13 Comparison between the experimental and the model weight fraction distribution for the experiment of (HAMIELEC; HODGINS; TEBBENS, 1967)

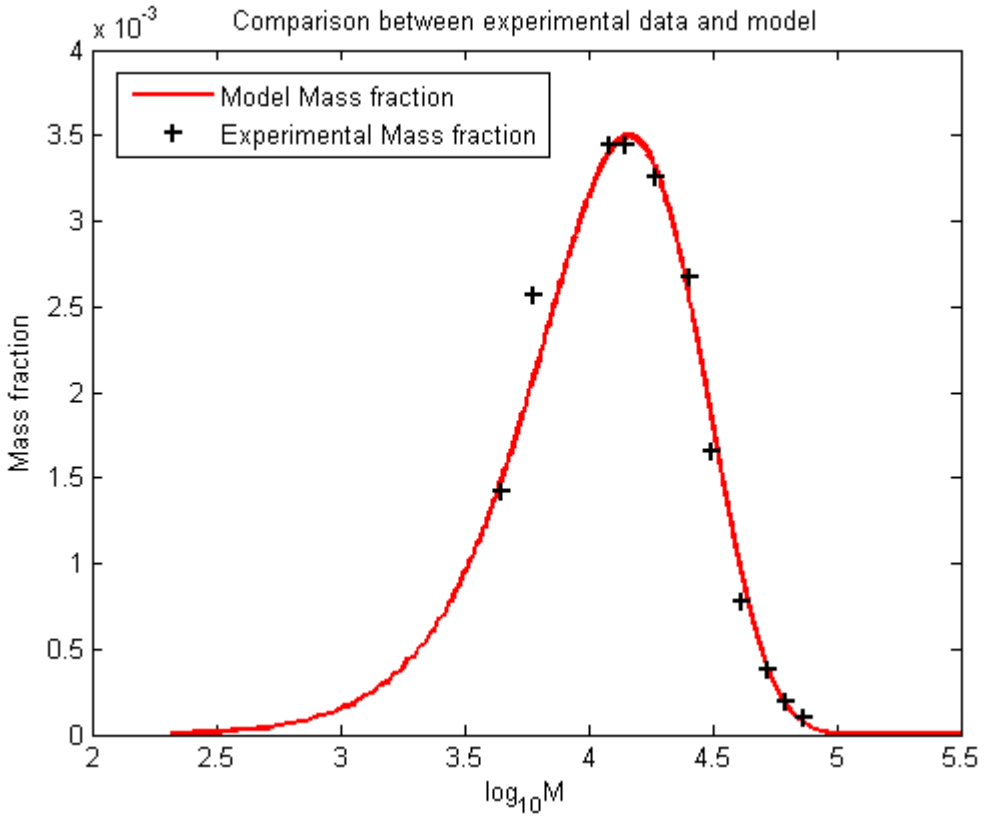

Source: (MELLONI, 2014)

3.6.1.2. Monomer 52% wt. (IWASAKI; YOSHIDA, 2005)

A batch reactor was charged with styrene and toluene using a monomer to solvent ratio of 51.7% wt. The initiator used was azobisisobutyronitrile (AIBN).

T [K]	P [atm]	Time [min]	M_0 [mol/L]	I_0 [mol/L]	S_0 [mol/L]
373.15	1	20	4.066	$4.066 \cdot 10^{-2}$	4.287

Table 8 Reaction conditions used by (IWASAKI; YOSHIDA, 2005).

The results of the simulated experiment are shown in Table 9 together with the experimental data.

α=0.1	M_N [g/mol]	M_W [g/mol]	Conversion
Experimental Result	5,600	9,520	0.386
Simulation Result	5,719	9,256	0.362

Table 9 Comparison between experimental results and model results.

Figure 3-14 and Figure 3-15 show the resulting molecular weight distribution for this experiment and the comparison between the predicted and the experimental M_N evolution along time.

Figure 3-14 Mass fraction distribution computed by the rigorous model for (IWASAKI; YOSHIDA, 2005)

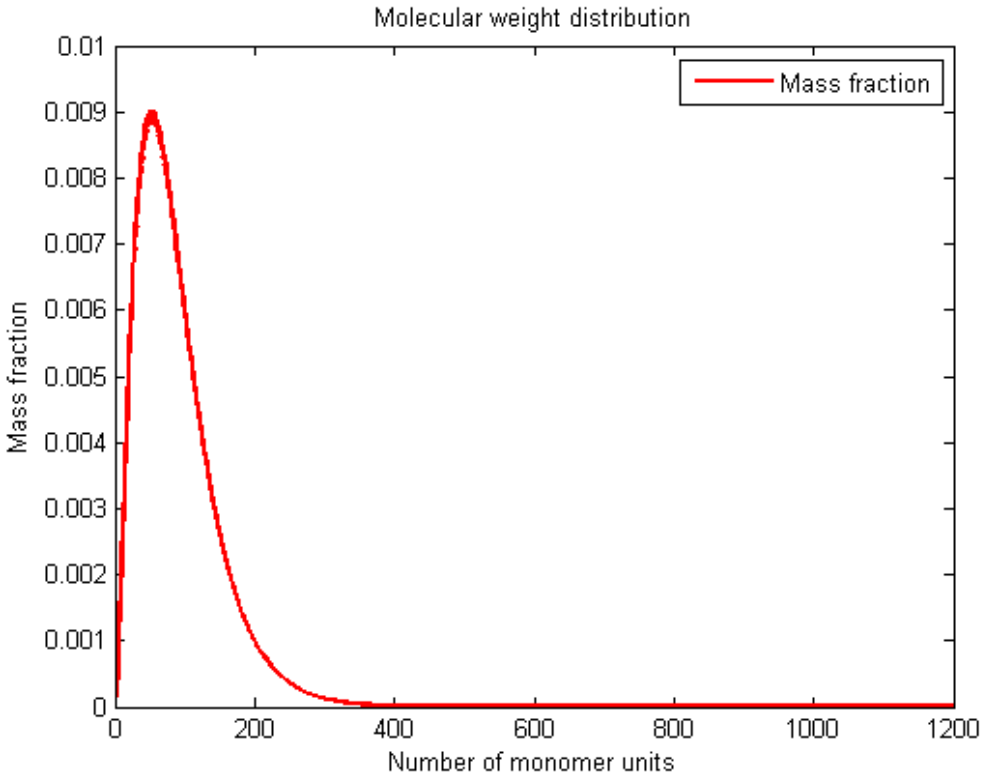

Source: (MELLONI, 2014)

Figure 3-15 Comparison between experimental and predicted M_N[6]

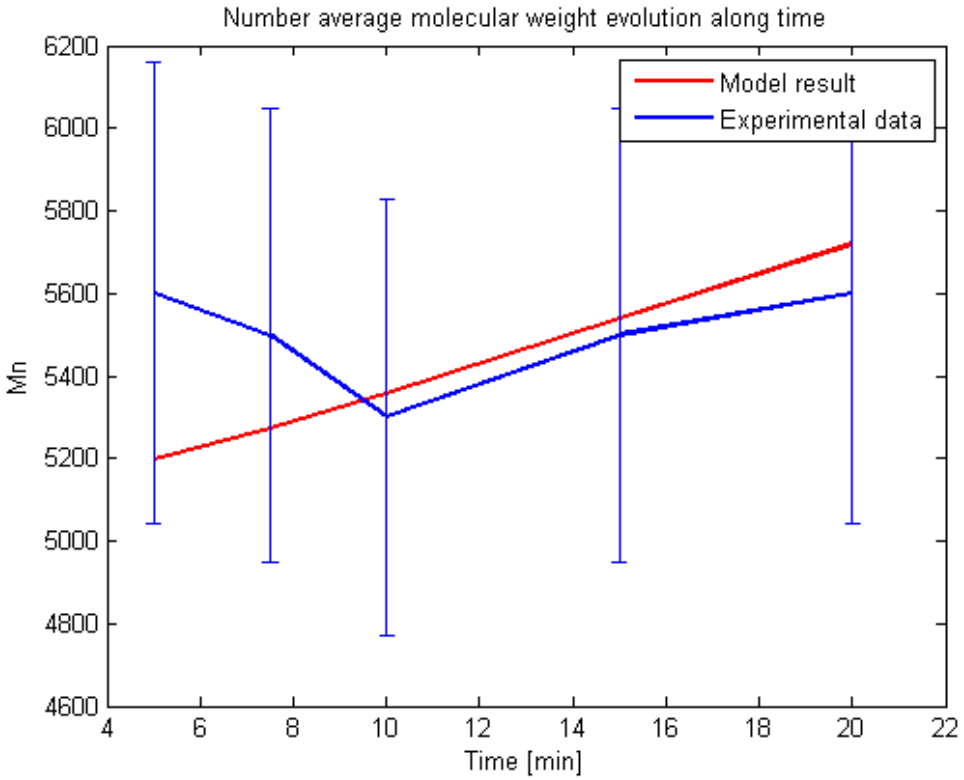

Source: (MELLONI, 2014)

3.6.1.3. Monomer 70% wt. (FONTOURA et al.*, 2003)*

As in the previous cases, the authors used a batch reactor. The monomer to solvent (toluene) ratio was 70% wt. and the initiator used is benzoyl peroxide.

T [K]	P [atm]	Time [min]	M_0 [mol/L]	I_0 [mol/L]	S_0 [mol/L]
364.15	1	420	6.007	$9.07 \cdot 10^{-3}$	2.878

Table 10 Reaction conditions used by (FONTOURA et al., 2003).

Table 11 shows the comparison between experimental and predicted results while Figure 3-16 shows the MWD relative to this experiment.

[6] Being that the author does not provide additional information on the gel permeation chromatography (GPC) experimental error, a typical error of 10% was assumed

α=0.095	M_N [g/mol]	M_W [g/mol]	Conversion
Experimental Result	52,922	N.A.	0.60
Simulation Result	52,993	92,107	0.57

Table 11 Comparison between experimental results and model results.

Figure 3-16 MWD computed by the rigorous model for the experiment of (FONTOURA et al., 2003)

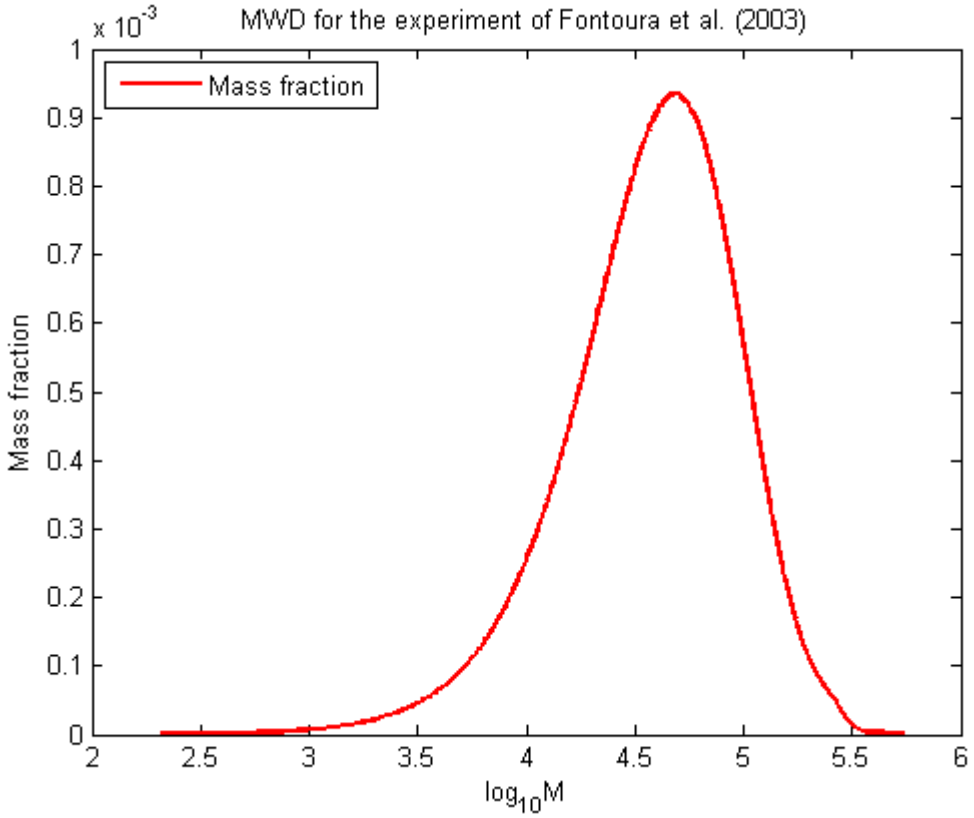

Source: (MELLONI, 2014)

3.6.1.4. Monomer 84% wt. (BOODHOO, 1999)

A batch reactor was charged with 200 ml of styrene, 40 ml of toluene and 3 g of benzoyl peroxide as initiator.

T [K]	P [atm]	Time [min]	M_0 [mol/L]	I_0 [mol/L]	S_0 [mol/L]
363.15	1	100	7.28	$5.17 \cdot 10^{-2}$	1.567

Table 12 Reaction conditions used by (BOODHOO, 1999).

Table 13, Figure 3-17, Figure 3-18, Figure 3-19 and Figure 3-20 summarize the comparison between experimental and model results. The best results were obtained using α=0.1. Notice that the conversion is slightly different, especially at the end of the reaction: this might be the effect of the temperature increase in the Boodhoo's experiment which, in fact, is not perfectly isothermal as the model is.

α=0.1	***M_N [g/mol]***	***M_W [g/mol]***	**Conversion**
Experimental Result	18,263	30,993	0.61
Simulation Result	18,817	30,773	0.56

Table 13 Comparison between experimental results and model results.

Figure 3-17 Molecular weight distribution computed by the rigorous model for the experiment of (BOODHOO, 1999)

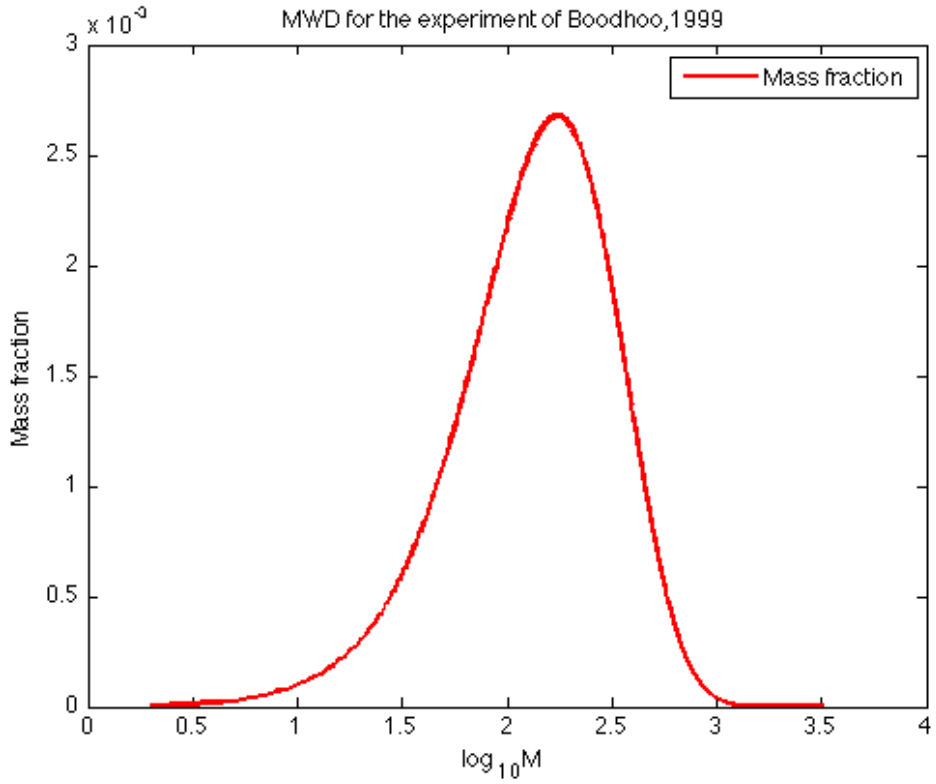

Source: (MELLONI, 2014)

Figure 3-18 Experimental and simulated conversion evolution along time

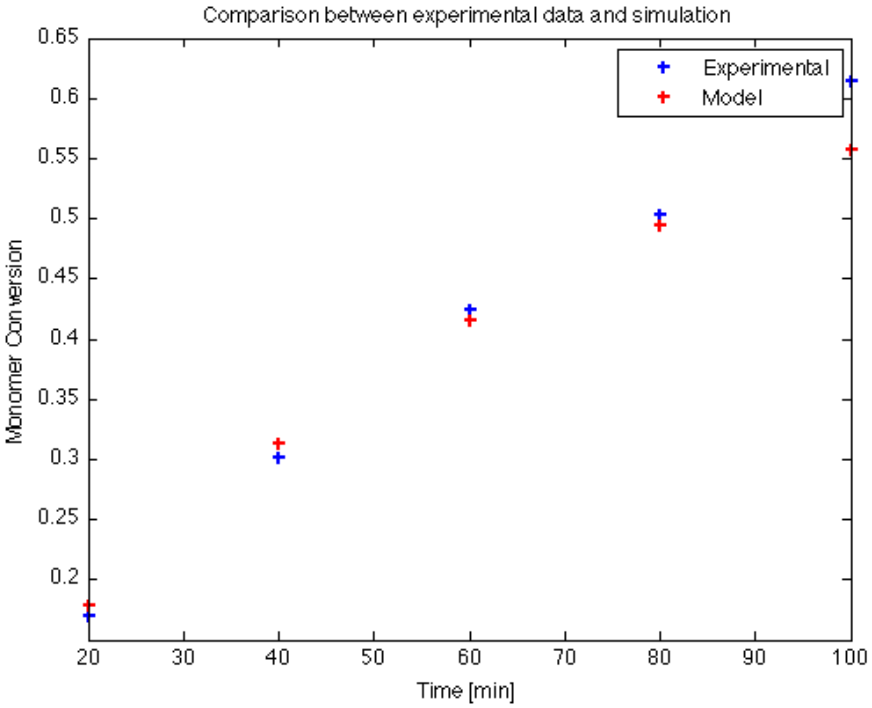

Source: (MELLONI, 2014)

Figure 3-19 Comparison between experimental and simulated MN evolution along time

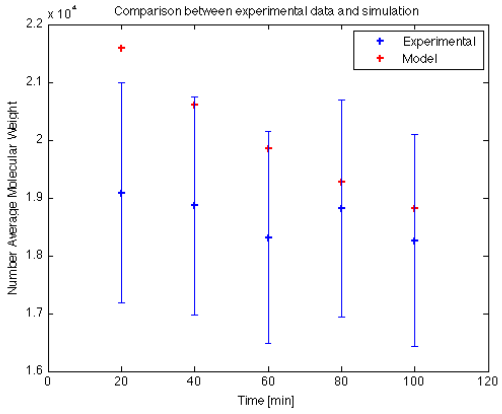

Source: (MELLONI, 2014)

Figure 3-20 Comparison between experimental and simulated MW evolution along time[7]

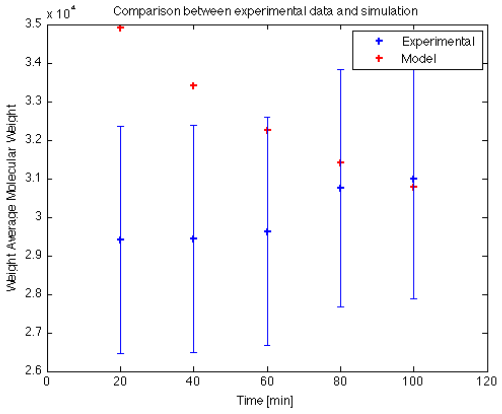

Source: (MELLONI, 2014)

3.6.2. Effects of the dilution over α.

In the previous section various experiments with different monomer to solvent ratios were compared to the predicted results of the model.

[7] Being that the author does not provide additional information on the gel permeation chromatography (GPC) experimental error, a typical error of 10% was assumed

Table 14 summarizes the effects of the dilution over the parameter α, remember that the values taken are the one which better represented the experimental data.

Monomer/Solvent [% wt.]	30	52	70	84
α	0.08	0.1	0.095	0.1

Table 14 Values for α which better represented the experimental data.

By comparing the values of α obtained for the different experiments, one can say that the dilution has practically no effects over the parameter α. The small fluctuations of this parameter can be easily explained with experimental errors (a GPC has typical experimental errors of 10%) and with different methods used to calculate the monomer conversion[8]. Considering that α should represent, in an empirical way, the diffusional limitations in the reacting mixture, the conclusion that can be drawn is that the termination mechanisms involved during the free radical polymerization of styrene are not affected by the dilution of the system.

3.7. Comparison with data from unconventional reactors

It is important to know how well the rigorous kinetic model succeeds in representing the experimental data obtained in unconventional reactors such as millireactors and microreactors. In order to do this, the data from various experiments (FULLIN, 2014) were compared to the results provided by the direct integration of the kinetic equations. The reactions were performed in a Syrris' microreactor model *ASIA120*. The reactor is a Teflon microtube with internal diameter of 500 μm and a total volume of 4 mL, coiled around a heating unit that allows temperatures from ambient up to 125°C. The feed enters in the reactor thanks to two syringe pumps having a flow rate range from 10 $\frac{\mu L}{min}$ up to 2 $\frac{mL}{min}$. The pumps draw fluid from a pressurized bottle which is maintained under nitrogen atmosphere, generating a slight overpressure, thus helping solvent and reagents to enter in the syringe pumps. The whole reacting system can be pressurized

[8] Frequently, the monomer conversion is calculated through empirical correlations based on the density of the solution and on its dilution (CABRAL, MELO, *et al.*, 2004).

thanks to a backpressure system located just before the reactor exit, allowing pressures up to 20 bar.

The reaction conditions are specified in Table 15.

Experiment Number	**Reactor Temperature [K]**	**Residence Time [min]**	**Solvent/Styrene %v.v.**	**Initiator** $[\frac{g}{100g}]$
1	373	5	60/40	1
2	373	20	60/40	1
3	373	20	60/40	2
4	373	20	60/40	0.5
5	373	40	40/60	1.5
6	373	40	40/60	1
7	373	80	40/60	1
8	373	80	40/60	0.2
9	388	80	30/70	1
10	388	80	30/70	0.5

Table 15 Rector's conditions for data comparison between experimental results and simulation results

After the reaction, measures of density are accomplished for calculating the conversion followed by a gel permeation chromatography in order to obtain parameters related to the polymer produced. A typical GPC result is showed in Figure 3-21.

Figure 3-21 Typical GPC measurement

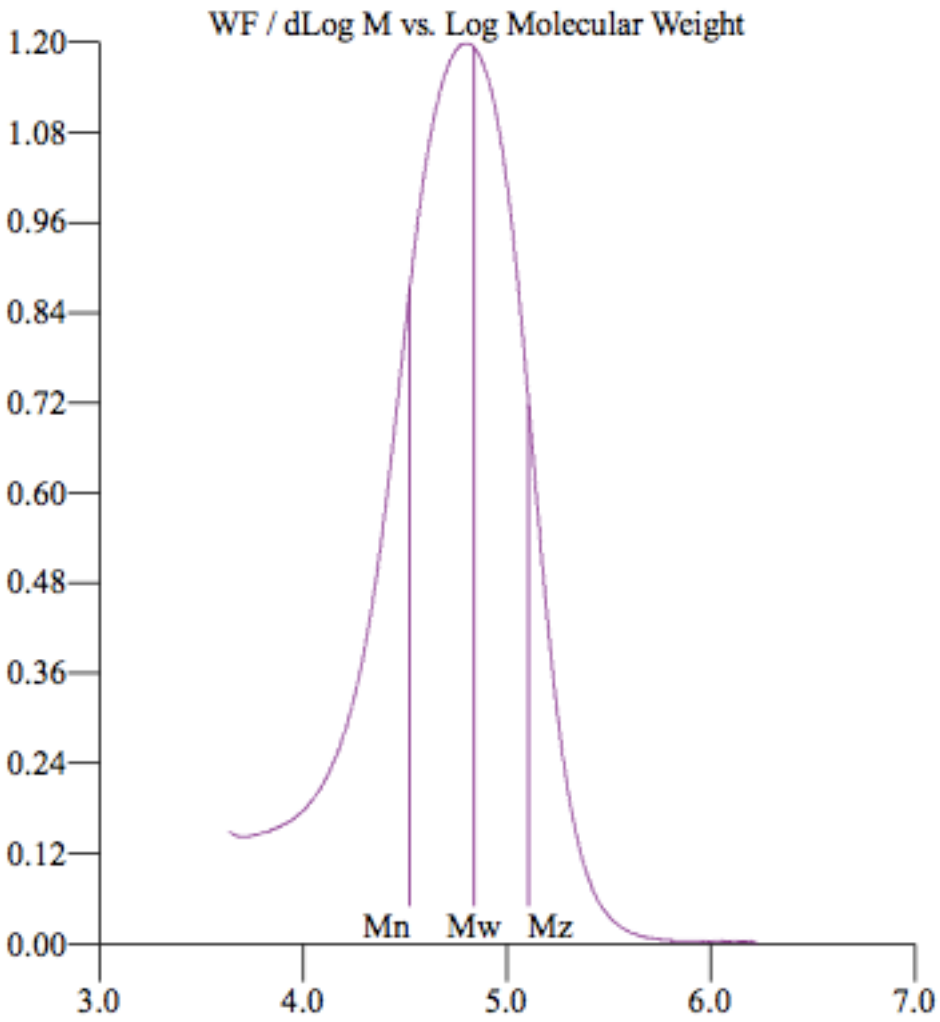

Source: (FULLIN, 2014)

Table 16 and in Table 17 show the comparison between experimental results and predicted results. In section 6.4 the MWD of the experimental results are compared to the predicted MWD. The value for the parameter α used in the model is set to 0.1.

Experiment Number	Experimental Conversion	Calculated Conversion
1	0.091	0.083
2	0.272	0.27
3	0.391	0.35
4	0.181	0.20
5	0.478	0.49
6	0.414	0.43
7	0.638	0.59
8	0.279	0.35
9	0.668	0.54
10	0.531	0.43

Table 16 Comparison between experimental conversion and calculated conversion.

Exp n°	Experimental M_N	Calculated M_N	Exp n°	Experimental M_W	Calculated M_W
1	6,768	8,279	**1**	10,626	13,307
2	6,587	8,212	**2**	11,857	13,203
3	5,640	5,347	**3**	8,234	8,562
4	11,531	12,448	**4**	19,372	20,109
5	8,907	9,632	**5**	17,101	15,507
6	9,255	12,689	**6**	20,824	20,636
7	13,786	13,172	**7**	25,642	21,396
8	31,077	39,175	**8**	56,249	66,777
9	14,735	12,548	**9**	31,607	27,581
10	21,415	20,013	**10**	46,471	45,224

Table 17 Comparison between experimental and calculated MN and MW.

As it is possible to see in Table 16, the conversion is well predicted for all the experiments, except for experiments 9 and 10, which were the ones driven with more aggressive conditions: higher temperature and lower dilution. The number average and weight average molecular weight were predicted correctly by the model, always by

considering a 10% error on the experimental data. Nevertheless, what is possible to see from the complete MWDs (section 6.4), is that the trend of the predicted MWD is to be always shifted to lower molecular weights compared to the experimental results.

The influence of the gel effect in such differences can be excluded with reasonable confidence: the maximum concentration of the monomer was 70% v/v and the higher conversion reached, considering all the experiments, was 63%. These conditions are not critical enough to lead to an important contribution of the gel effect. The reasons of these differences must be sought elsewhere.

Although the model involves the rigorous integration of the kinetic equations, some simplifications still remain. The usage of a millireactor involves a special fluid dynamics and the equipment cannot be considered as an ideal plug flow reactor. In such a reactor there are internal mixings and diffusional effects (ZHANG et al., 2006) that may affect the polymerization mechanisms and, consequently, the final polymer properties. Those effects are not considered in the model used to predict the reaction results and this might be the principal motivation of the discrepancy between the predicted and the effective MWDs.

It will thus be important to characterize these events and try to understand how it is possible to take into account these non-idealities in the computational treatment.

Chapter 4. Rigorous Computation of the Molecular Weight Distribution for a Methyl Methacrylate Polymerization

As it has been done for the styrene polymerization, the methyl methacrylate polymerization was studied with the aim of analyzing the same aspects of the styrene polymerization: computational time for the implementation of the system and termination mechanism.

The two reactions can be considered similar and different: the systems react with the same mechanism, following a reaction path common to all the free radical polymerizations. However, the involved species have a different chemical nature, a different termination mechanism and different diffusional limitations.

The objective of this chapter, in contrast with the polystyrene studies, will not be to determine how the dilution influences the interactions between the long-chain radicals but, due to the importance of the gel-effect in the MMA polymerization, it will instead be to try to suggest how the macroradical interactions can be taken into account in a model that considers every single radical species.

4.1. Equations for the polymethyl methacrylate

The balance equations derived from the kinetic scheme of the methyl methacrylate polymerization are:

- Initiator

$$\frac{dI}{dt} = -k_d I \qquad \textbf{Eq. 33}$$

- Initiator's radical

$$\frac{dR^*}{dt} = 2fk_d I - k_i R^* M \qquad \textbf{Eq. 34}$$

- Monomer

$$\frac{dM}{dt} = -k_i R^* M - k_p M \sum_{i=1}^{\infty} P_i^* + k_{fs} S P_1^* - k_{fm} M \sum_{i=2}^{\infty} P_i^* \qquad \textbf{Eq. 35}$$

- Monomer's radical

$$\frac{dP_1^*}{dt} = k_i R^* M - k_p P_1^* M - P_1^* \sum_{i=1}^{\infty} k_{tc}(1,i) P_i^* + \left(k_{fs} S + k_{fm} M\right) \sum_{i=2}^{\infty} P_i^* \qquad \textbf{Eq. 36}$$

- Polymer's radical

$$\frac{dP_n^*}{dt} = k_p P_{n-1}^* M - k_p P_n^* M - P_n^* \sum_{i=1}^{\infty} k_{tc}(n,i) P_i^* - \left(k_{fs} S + k_{fm} M\right) P_n^* \quad n \geq 2 \quad \textbf{Eq.37}$$

- Dead polymer

$$\frac{dD_n}{dt} = P_n^* \sum_{i=1}^{\infty} k_{tc}(n,i) P_i^* + \left(k_{fs} S + k_{fm} M\right) P_n^* \quad \textbf{Eq. 38}$$

The direct integration criteria are the same for the polystyrene model, explained in section 3.1.1.

4.1.1. Computational implementation of the gel effect in the termination rate constant

As it is written in section 2.1.2, three types of models are used to describe the gel effect for the methyl methacrylate polymerization: mechanistic, semi-empirical and fully empirical. However, it appears in literature that the semi-empirical models are the most used. This can be explained by the fact that they combine ease of implementation with the ability to generalize the results to other systems. The mechanistic models are much more difficult to be developed and to be used (SCHMIDT; RAY, 1981), while the fully empirical models can be unreliable when extrapolating the results to systems with different operating conditions such as varying dilution or temperature.

The model proposed is an analogy of the one developed by Schmidt and Ray (1981), extended to a variable termination rate for every radical combination:

$$k_{tc} = \begin{cases} \left[\textbf{if } V_f > V_{fcr}\right] \dfrac{k_{tc0}}{(ij)^{\exp(-\alpha V_f)}} \\ \left[\textbf{if } V_f \leq V_{fcr}\right] \dfrac{k_{tc0}}{(ij)^{\exp\{-\alpha V_{fcr} + \beta (V_{fcr} - V_f)\}}} \end{cases}$$

$$V_{fcr} = 0.1856 - 2.965 \cdot 10^{-4}(T - 273.2)$$

$$V_f = V_{fp}\varphi_p + V_{fm}\varphi_m + V_{fs}\varphi_s$$

$$V_{fp} = 0.025 + \alpha_p (T - T_{gp})$$

$$V_{fm} = 0.025 + \alpha_m (T - T_{gm})$$

$$V_{fs} = 0.025 + \alpha_s (T - T_{gs})$$

Here, α and β are two parameters and *i*, *j* are the relative length of the interacting radicals.

The estimation of α and β is made by minimizing the difference between the conversion given by the model and the experimental conversion taken from Schultz and Harborth (1947). These authors studied the methyl methacrylate polymerization in bulk and in a solution of benzene at various concentrations and temperatures (Figure 2-3 and Figure 4-1).

Figure 4-1 Data for MMA polymerization in benzene at 70°C, [BPO]=10 g/L. (1) [MMA] bulk. (2) [MMA]=80%v/v. (3) [MMA]=60%v/v. (4) [MMA]=40%v/v. (5) [MMA]=20%v/v

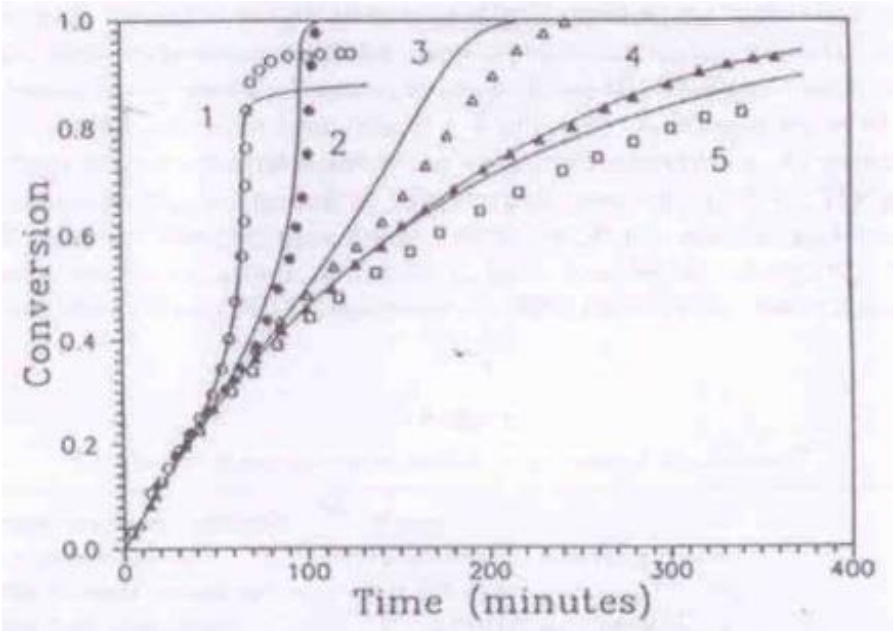

Source: (SCHULTZ; HARBORTH, 1947)

4.1.2. Estimation of the parameters α and β

What it is possible to see from Figure 2-3 and Figure 4-1 is that at low conversions (approximately up to 20-25% for a temperature of 70°C and 10% for a temperature of 50°C) the dilution does not affect the conversion evolution along time. Furthermore, for how the gel-effect model was conceived, α describes the termination only before the overall free volume of the reaction reaches the critical value and β describes the termination only after reaching the critical conditions. This allows one to split the multidimensional minimization into two one-dimensional minimizations: a first estimation of the parameter α is made considering only the conversion data obtained at

the beginning of the reaction. Afterwards, α is maintained as a fixed value and the estimation of β is computed considering all the conversion data.

To estimate α, the data related to the curve 1 of Figure 4-1 is used. Once estimated the value of α, the reaction conditions are varied in order to match those of the curves 1, 2, 3 and 5. This is made to confirm that all the predicted conversions will follow the same trend at the beginning of the reaction (at low conversion).

The kinetic constants used for this simulation are taken from Tobolsky and Baysal (1953), Mahabadi and O'Driscoll (1977) and Marten and Hamielec (1979). They were all used together by Schmidt and Ray (1981) and are listed in Table 18. The termination rate constant between two monomers is taken from Barner-Kowollik and Russell (2009) and varies according to the temperature.

Dissociation constant	k_d *[1/s]*	$1.69 * 10^{14} exp\left(\frac{-15098}{T}\right)$
Propagation constant	k_p *[L/mol/s]*	$4.92 * 10^{5} exp\left(\frac{-2191}{T}\right)$
Monomer chain transfer constant	k_{fm} *[L/mol/s]*	0.043
Solvent chain transfer constant	k_{fs} *[L/mol/s]*	*Depends on the solvent*

Table 18 Kinetic constants used for the MMA polymerization model

The results given by the model are showed in Figure 4-2 and Table 19 reports the optimized values for α and β.

Experiment	Dilution [v.v%]	Temperature [°C]	α	β
1 (magenta)	Bulk (0%)	70	7.5	11
2 (black)	80%	70	5.0	N.A.
3 (red)	20%	50	7.5	12
4 (blue)	80%	50	6.0	N.A.

Table 19 Estimated values of α and β for various experiments

The values for β in the case of high-dilution is not available due to the fact that, for the criteria used, such reactions never reached the critical free volume value and, consequently, only the parameter α was sufficient to describe the conversion trend.

Figure 4-2 Conversion evolution along time for various MMA polymerizations

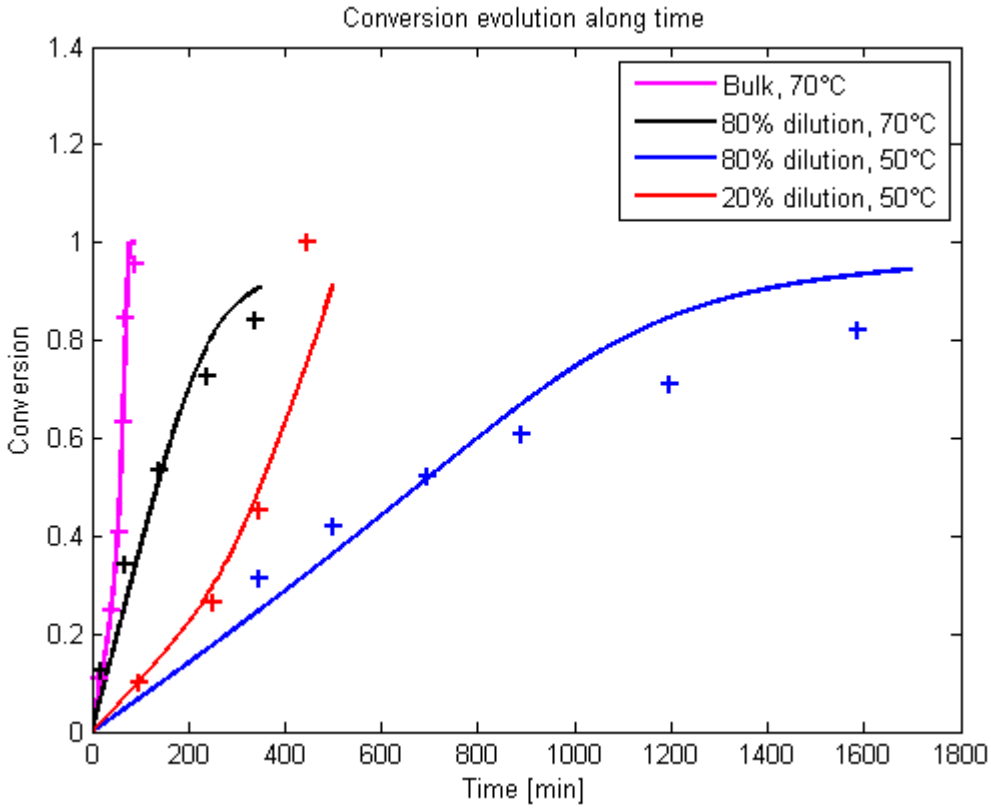

Source: (MELLONI, 2014)

The MWDs for the reactions at 20% dilution are showed in Figure 4-3:

Figure 4-3 MWD for different reaction temperature and 80% dilution v.v%

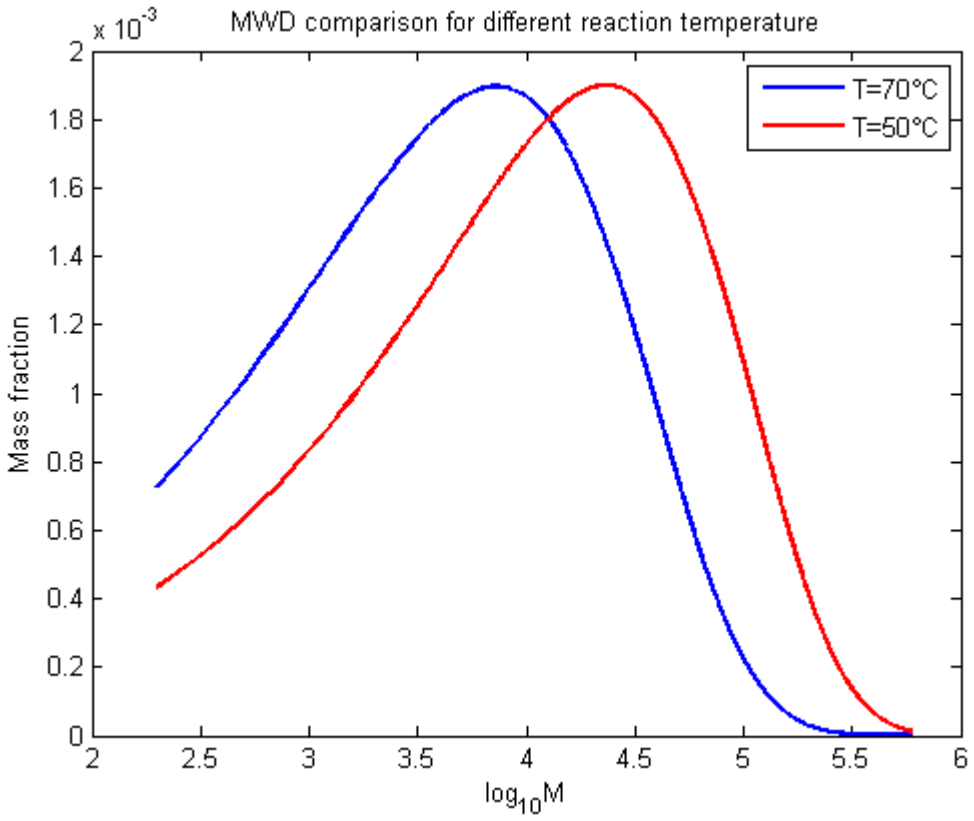

Source: (MELLONI, 2014)

Temperature	Reaction time	Conversion	M_N [g/mol]	M_W [g/mol]	PD
50 °C	1700 min	0.95	31,136	112,255	3.61
70 °C	350 min	0.91	11,946	46,525	3.89

Table 20 Conversion, MN and MW predicted by the model for the experiments with 80% dilution

Figure 4-2 shows a good accordance between the model predictions and the experimental points. Moreover, what it is possible to observe with respect to the parameter α is that as long as the dilution increases, the parameters tends to decrease. This can be justified by the fact that, for high dilutions, the conversion rise at the beginning of the reaction should be less pronounced but, as a matter of fact, Figure 2-3 and Figure 4-1 show that for low conversions, all the conversion trends have the same slope, regardless of the dilution. This imposes a higher dependence on the radical chain

length for the termination rate constant at high dilutions (note that, if α decrease, the dependence on the radical chain length increases). It is important to highlight that the parameter introduced to describe the gel effect is β and, as a consequence, this does not mean that the gel effect is more pronounced at high dilutions (which would be hardly explainable).

Chapter 5. Conclusions and further studies

The aim of the work was to obtain the complete molecular weight distribution for free-radical polymerizations and to study the Norrish-Trommsdorff effect over the termination rate constant. The very first step was setting-up the system concerning a styrene polymerization and implement it on the MATLAB numerical computing environment. Due to the very high computational time requirements, some efforts have been made in order to reduce the time requirements. Besides demonstrating that averaging the termination rate constant using the radical molar fractions would reduce the computational time requirements without affecting dramatically the MWD, remarkable results were obtained thanks to the implementation of the Jacobian matrix. A correlation found in literature and suitable to a model that takes into account every single radical species was used to describe the gel-effect into the styrene polymerization. Comparison with experimental data showed that the dilution of the reaction system does not affect the termination rate constant diminution related to the Norrish-Trommsdorff effect: all the experimental data were fitted using the same correlation and the same parameter α. Moreover, exploiting this result, an attempt to describe experimental data obtained from an unconventional millireactor was made. The results appeared to be quite satisfactory despite the fact that the molecular weight distributions predicted by the model were always shifted to lower molecular weights when compared to the GPC data. Afterwards, the study focused on the methyl methacrylate polymerization, which presented a gel-effect much stronger compared to the polystyrene systems. It appeared that the correlation used to describe the styrene's termination rate constant dependence with the radical length was not able to describe properly the MMA polymerization. Studying the literature revealed that the best way to describe the termination chain-length dependence was through semi-empirical correlations. Therefore, a correlation was chosen and adapted to be employed in the model used in this work. The comparison with experimental results showed a reasonable agreement, even if some important deviations were observed.

For the future, two principal objectives should be contemplated: accuracy of the predictions and time requirements. The former is obviously in the interest of having predictions more and more accurate, able to correctly forecast all the important parameters of the reaction like conversion and MWD. This would be of great interest

even to other branches of study such as computational fluid dynamics; this would give the possibility to build more complex models, capable of describing the fluid dynamics during a polymerization reaction, which is still a topic extensively studied at the present. Directly related to this, for live-monitoring applications and for the computation of distributions shifted to higher molecular weights, the computational time is still being a limiting factor that could be overcome by fixing computational inefficiencies. Such inefficiencies may occur in code sections that can be conceived in a more efficient way; otherwise they may be intrinsically related to the system that is been computed and, in this case, solutions like parallelization of the calculations over different processors would speed up the computational time.

Chapter 6. Appendix

6.1. Analytical derivation of the Jacobian matrix for the polystyrene system

The Jacobian matrix is the matrix containing all the first order partial derivatives of the system.

$$J = \begin{bmatrix} \frac{\partial f_1}{\partial x_1} & \cdots & \frac{\partial f_1}{\partial x_n} \\ \vdots & \ddots & \vdots \\ \frac{\partial f_n}{\partial x_1} & \cdots & \frac{\partial f_n}{\partial x_n} \end{bmatrix}$$

For the styrene polymerization, the kinetic scheme can be divided into various parts, each one showing special logical patterns for the computational implementation.

6.1.1. Initiator equation

$$\frac{dI}{dt} = -k_d I$$

The only non-negative derivative is the one made with respect to the initiator concentration *I*.

6.1.2. Monomer equation

$$\frac{dM}{dt} = -k_i R^* M - k_p M \sum_{i=1}^{\infty} P_i^* + k_{fs} S P_1^* - k_{fm} M \sum_{i=2}^{\infty} P_i^*$$

The derivatives made with respect to the initiator concentration *I*, the monomer concentration *M* and the monomeric radical P_1^* must be implemented individually.

$$\frac{\partial \left(\frac{dM}{dt}\right)}{\partial I} = -2 f k_d$$

$$\frac{\partial\left(\frac{dM}{dt}\right)}{\partial M} = -k_p \sum_{i=1}^{\infty} P_i^* - k_{fm} \sum_{i=2}^{\infty} P_i^*$$

$$\frac{\partial\left(\frac{dM}{dt}\right)}{\partial P_1^*} = -k_p M + k_{fs} S$$

The derivatives concerning the polymeric radicals are all equal:

$$\frac{\partial\left(\frac{dM}{dt}\right)}{\partial P_n^*} = -k_p M - k_{fm} M$$

Finally, the derivatives with respect to the dead polymer are all equal to zero.

6.1.3. Monomeric radical

$$\frac{dP_1^*}{dt} = k_i R^* M - k_p P_1^* M - P_1^* \sum_{i=1}^{\infty} k_{tc}(1,i) P_i^* + \left(k_{fs} S + k_{fm} M\right) \sum_{i=2}^{\infty} P_i^*$$

Once again, the derivatives made with respect to the initiator concentration *I*, the monomer concentration *M* and the monomeric radical P_1^* must be written individually.

$$\frac{\partial\left(\frac{dP_1^*}{dt}\right)}{\partial I} = 2 f k_d$$

$$\frac{\partial\left(\frac{dP_1^*}{dt}\right)}{\partial M} = -k_p P_1^* + k_{fm} \sum_{i=2}^{\infty} P_i^*$$

$$\frac{\partial\left(\frac{dP_1^*}{dt}\right)}{\partial P_1^*} = -k_p M - 2k_{tc}(1,1) P_1^* - \sum_{j=2}^{\infty} k_{tc}(1,j) P_j^*$$

The derivatives made with respect to the polymeric radicals can be expressed as it follows:

$$\frac{\partial\left(\frac{dP_1^*}{dt}\right)}{\partial P_k^*} = -k_{tc}(1,k) P_1^* + k_{fs} S + k_{fm} M$$

All the derivatives made with respect to the dead polymer are equal to zero.

6.1.4. Polymeric radicals

$$\frac{dP_n^*}{dt} = k_p P_{n-1}^* M - k_p P_n^* M - P_n^* \sum_{i=1}^{\infty} k_{tc}(n,i) P_i^* - \left(k_{fs} S + k_{fm} M\right) P_n^*$$

The derivatives made with respect to *I* and *M* are written individually.

$$\frac{\partial \left(\frac{dP_n^*}{dt}\right)}{\partial I} = 0$$

$$\frac{\partial \left(\frac{dP_n^*}{dt}\right)}{\partial M} = k_p P_{n-1}^* - k_p P_n^* - k_{fm} P_n^*$$

When deriving with respect to the radicals (including the monomeric radical), it is convenient to distinguish three different cases.

$$\frac{\partial \left(\frac{dP_n^*}{dt}\right)}{\partial P_k^*}$$

$$= \begin{cases} [\boldsymbol{if\ k = n-1}] \rightarrow k_p M - k_{tc}(n,k) P_n^* \\ [\boldsymbol{if\ k = n}] \rightarrow -k_p M - 2P_n^* k_{tc}(n,n) - \sum_{j=1}^{n-1} k_{tc}(n,j) P_j^* - \sum_{j=n+1}^{\infty} k_{tc}(n,j) P_j^* - k_{fs} S - k_{fm} M \\ [\boldsymbol{else}] \rightarrow -k_{tc}(n,k) P_n^* \end{cases}$$

Finally, the derivatives with respect to the dead polymer are all equal to zero.

6.1.5. Dead polymer

$$\frac{dD_n}{dt} = \frac{1}{2} \sum_{i=1}^{\infty} k_{tc}(i, n-i) P_i^* P_{n-i}^* + \left(k_{fs} S + k_{fm} M\right) P_n^*$$

Similarly to the polymeric radicals derivatives, only the derivatives made with respect to *I* and *M* are written individually.

$$\frac{\partial\left(\frac{dD_n}{dt}\right)}{\partial I} = 0$$

$$\frac{\partial\left(\frac{dD_n}{dt}\right)}{\partial M} = k_{fm}P_n^*$$

When deriving with respect to the radicals, three different cases appear.

$$\frac{\partial\left(\frac{dD_n}{dt}\right)}{\partial P_k^*} = \begin{cases} [\boldsymbol{if}\ \boldsymbol{k} > n] \rightarrow 0 \\ [\boldsymbol{if}\ \boldsymbol{k} = \boldsymbol{n}] \rightarrow k_{fs}S + k_{fm}M \\ [\boldsymbol{if}\ \boldsymbol{k} < n] \rightarrow P_{n-k}^* \end{cases}$$

Just as for the other cases, the derivatives with respect to the dead polymer are equal to zero.

6.2. Analytical derivation of the Jacobian matrix for the polymethyl methacrylate system

Basically, the only difference between the styrene polymerization is the termination mechanism via disproportionation. Consequently, the derivatives applied to the functions regulating the variations of the initiator, monomer and radicals are exactly the same as the styrene.

6.2.1. Dead polymer

$$\frac{dD_n}{dt} = P_n^* \sum_{i=1}^{\infty} k_{tc}(n,i)P_i^* + \left(k_{fs}S + k_{fm}M\right)P_n^*$$

The derivatives with respect to the initiator and the monomer are written individually.

$$\frac{\partial\left(\frac{dD_n}{dt}\right)}{\partial I} = 0$$

$$\frac{\partial\left(\frac{dD_n}{dt}\right)}{\partial M} = k_{fm}P_n^*$$

For the derivatives with respect to the radicals, similarly to the styrene's Jacobian, three cases appear.

$$\frac{\partial\left(\frac{dD_n}{dt}\right)}{\partial P_k^*} = \begin{cases} [\boldsymbol{if}\ \boldsymbol{k} > n] \rightarrow 0 \\ [\boldsymbol{if}\ \boldsymbol{k} = \boldsymbol{n}] \rightarrow \sum_{i=1}^{n-1} k_{tc}(n,i)P_i^* + \sum_{i=n+1}^{\infty} k_{tc}(n,i)P_i^* + 2k_{tc}(n,n)P_n^* + k_{fm}M + k_{fs}S \\ [\boldsymbol{if}\ \boldsymbol{k} < n] \rightarrow k_{tc}(n,k)P_n^* \end{cases}$$

6.3. Numerical methods for stiff ODEs systems

6.3.1. Backward differentiation formulas (BDFs)

The formulas give an approximation to a derivative of a variable at a specific time t_n, using the values of its function $y(t)$ at t_n and earlier times (GEAR, 2007). They are derived using the *k*-th degree interpolating polynomial which approximates the function $y(t)$ using $y(t_n), y(t_{n-1}), \ldots, y(t_{n-k})$.

Note that using a linear interpolating polynomial one obtains the Backward Euler method.

6.3.2. Numerical differentiation formulas (NDFs)

Being that high-order BDFs present poor stability, the NDFs have been introduced to improve the stability of the high-order BDFs (SHAMPINE; REICHELT, 1997).

6.4. MWD for the millireactor experiments

Here follows the comparison between experimental data and predicted data for the styrene polymerization in millireactors.

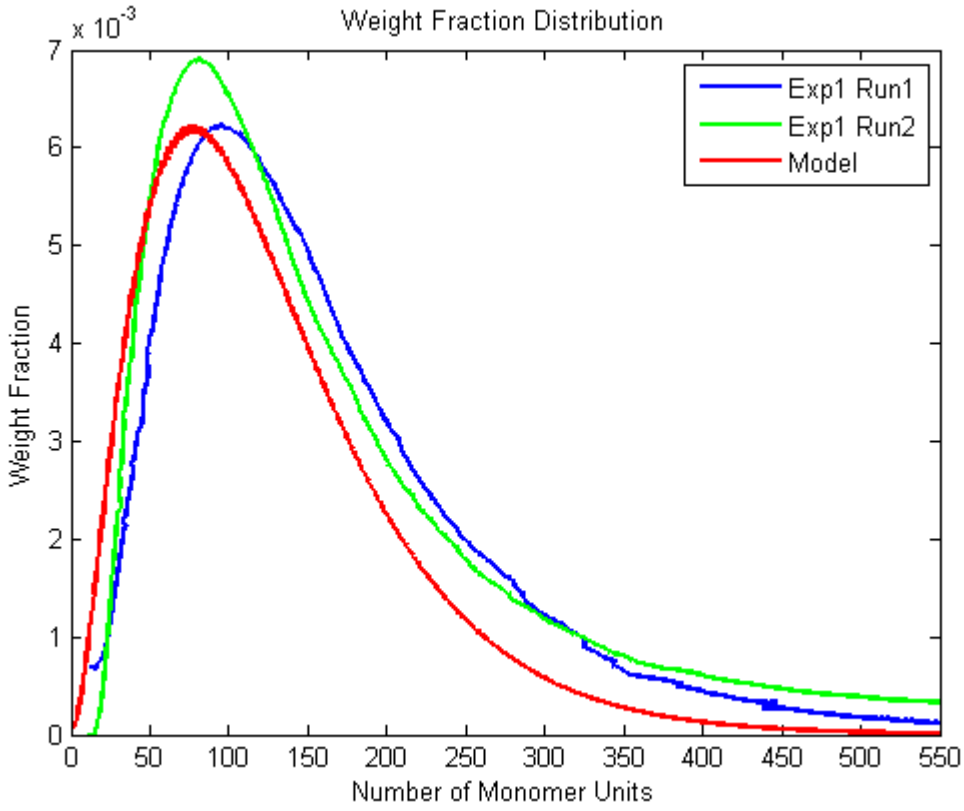
Weight Fraction Distribution
x 10^-3
Weight Fraction
Number of Monomer Units
Exp1 Run1
Exp1 Run2
Model
0
1
2
3
4
5
6
7
0
50
100
150
200
250
300
350
400
450
500
550

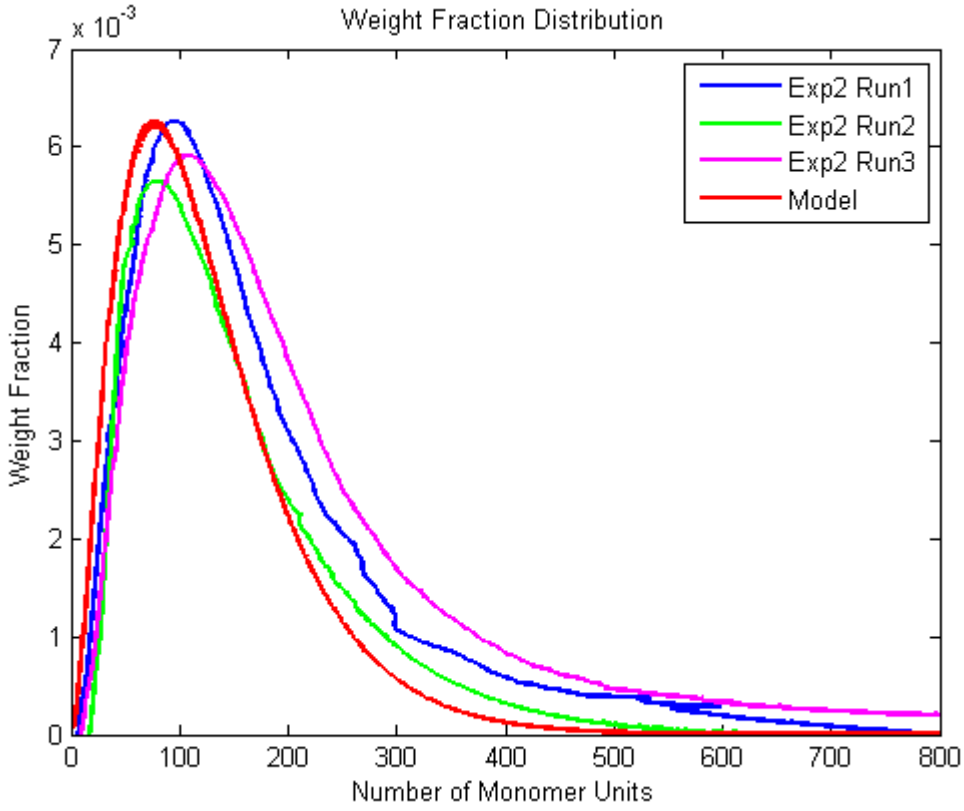
Weight Fraction Distribution
x 10^-3
Weight Fraction
Number of Monomer Units
Exp2 Run1
Exp2 Run2
Exp2 Run3
Model
0
1
2
3
4
5
6
7
0
100
200
300
400
500
600
700
800

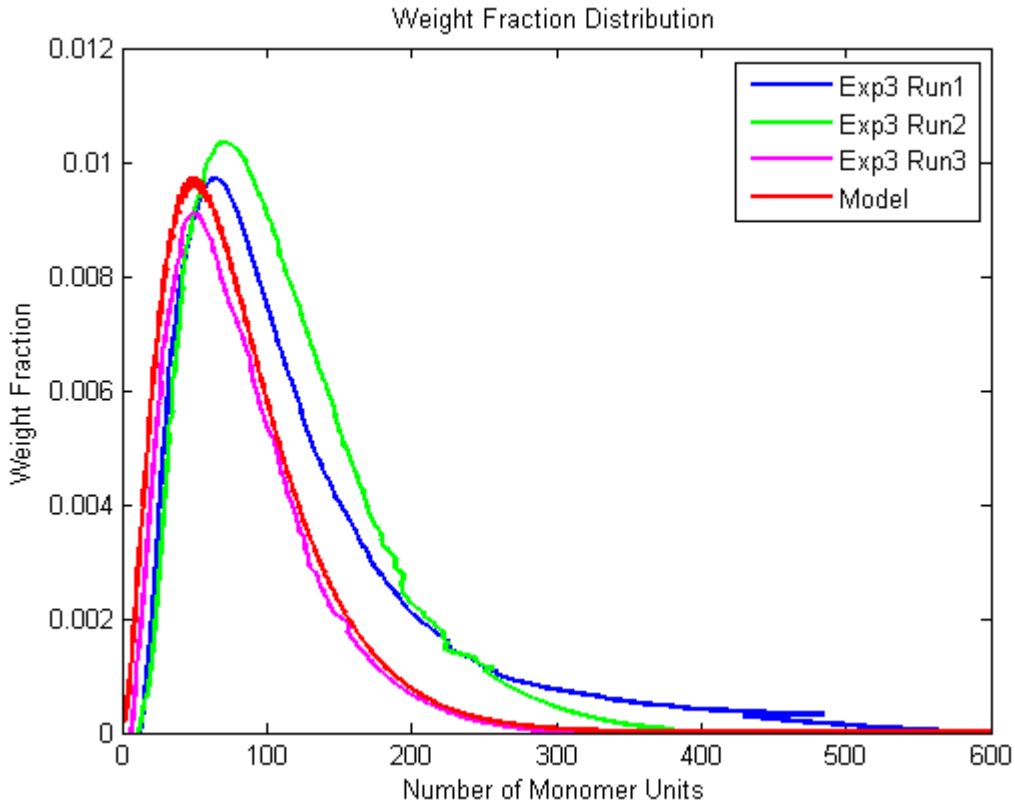
Weight Fraction Distribution
Exp3 Run1
Exp3 Run2
Exp3 Run3
Model
Weight Fraction
Number of Monomer Units
0.012
0.01
0.008
0.006
0.004
0.002
0
0
100
200
300
400
500
600

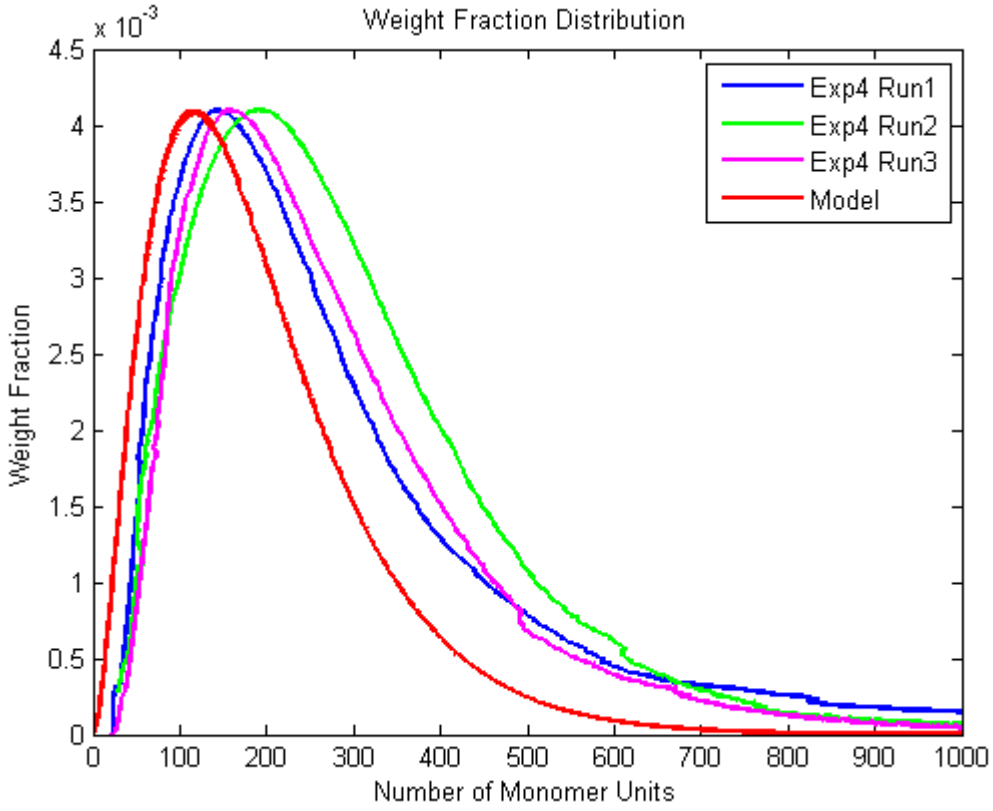
Weight Fraction Distribution
x 10^-3
Exp4 Run1
Exp4 Run2
Exp4 Run3
Model
Weight Fraction
Number of Monomer Units
4.5
4
3.5
3
2.5
2
1.5
1
0.5
0
0
100
200
300
400
500
600
700
800
900
1000

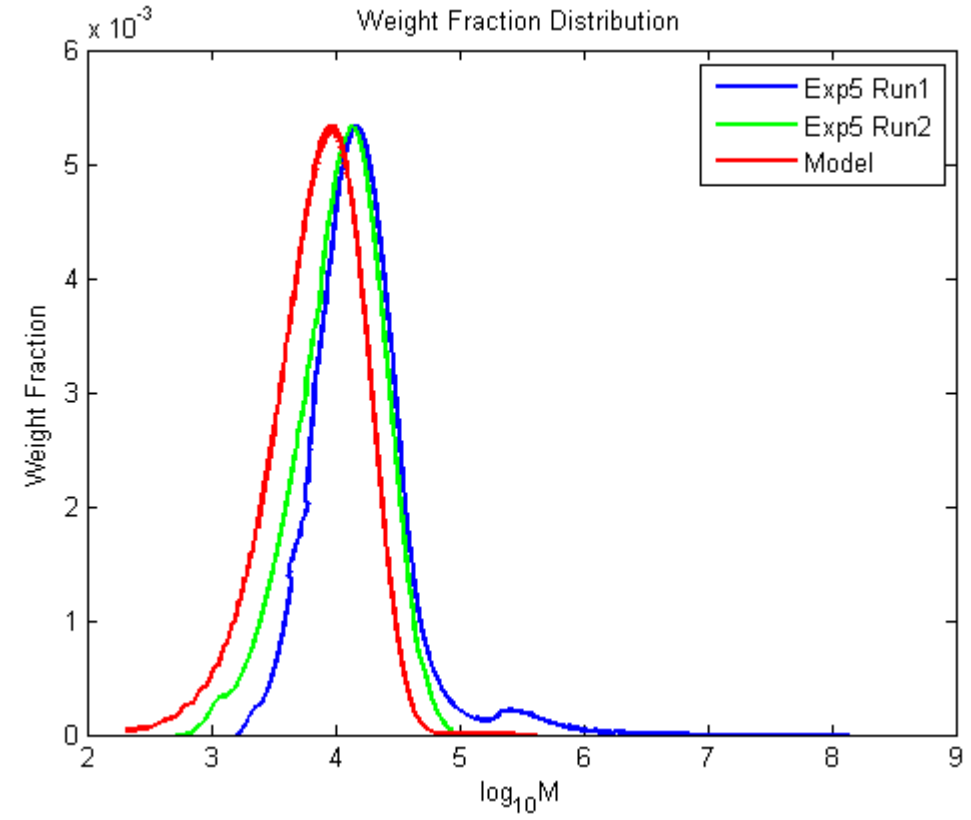
Weight Fraction Distribution
x 10^-3
Weight Fraction
log10M
Exp5 Run1
Exp5 Run2
Model

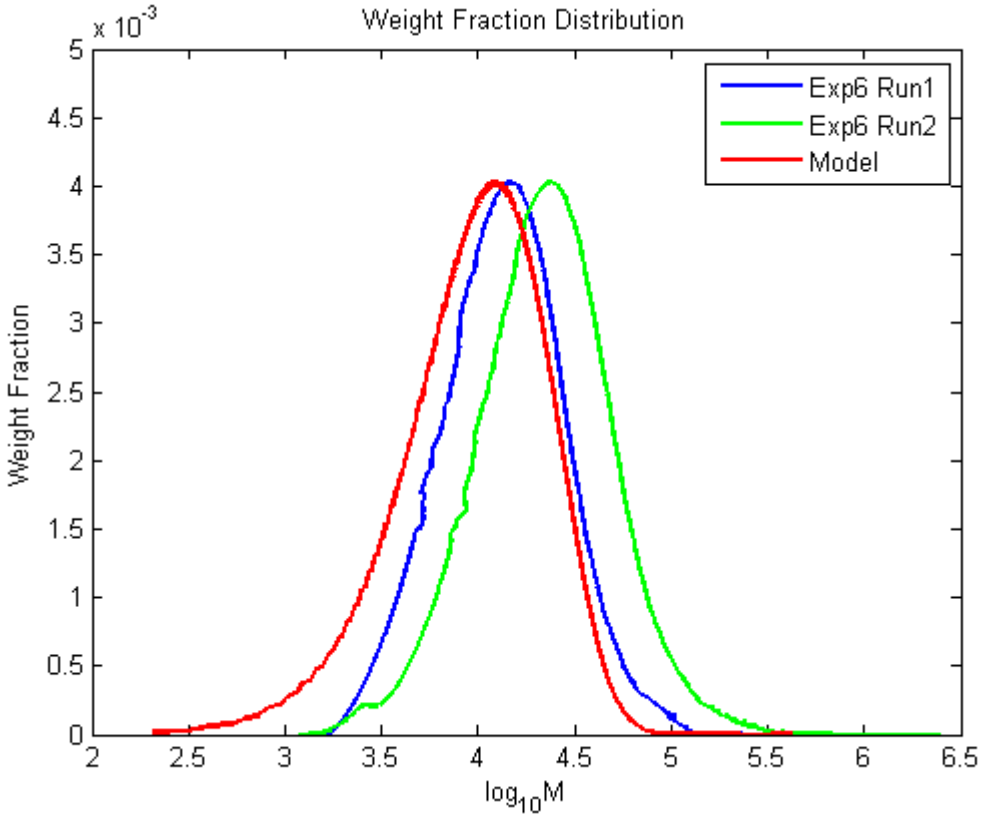
Weight Fraction Distribution
x 10^-3
Weight Fraction
log10M
Exp6 Run1
Exp6 Run2
Model

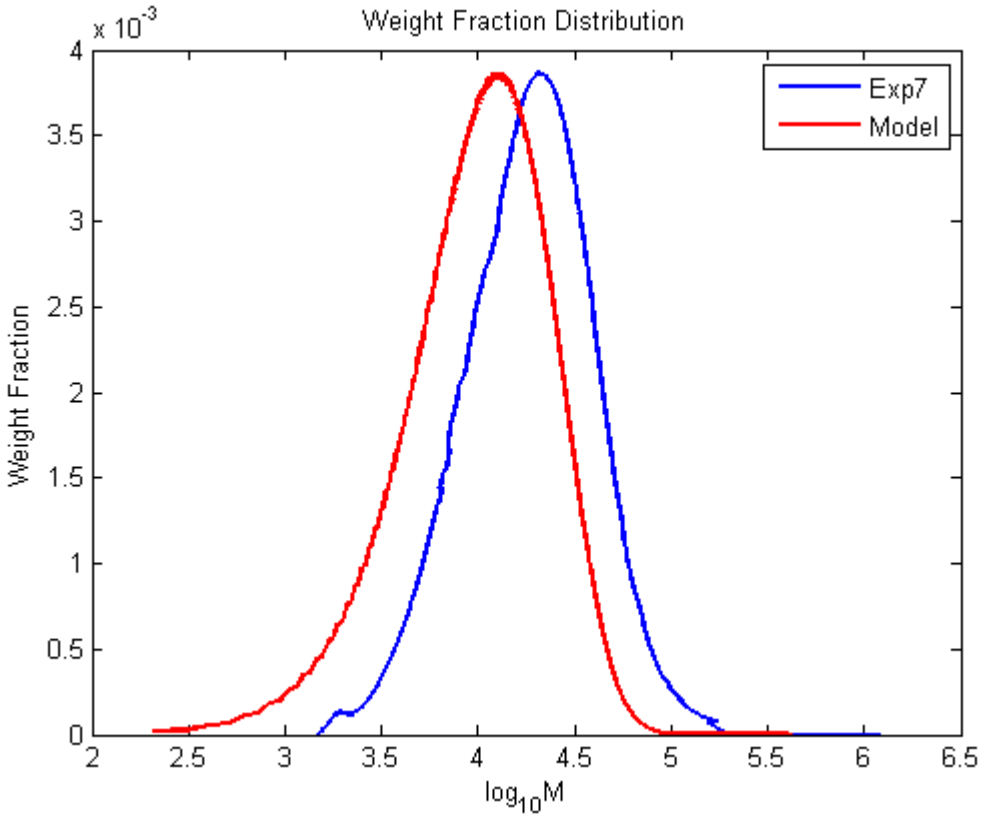
Weight Fraction Distribution
x 10^-3
Weight Fraction
log10M
Exp7
Model

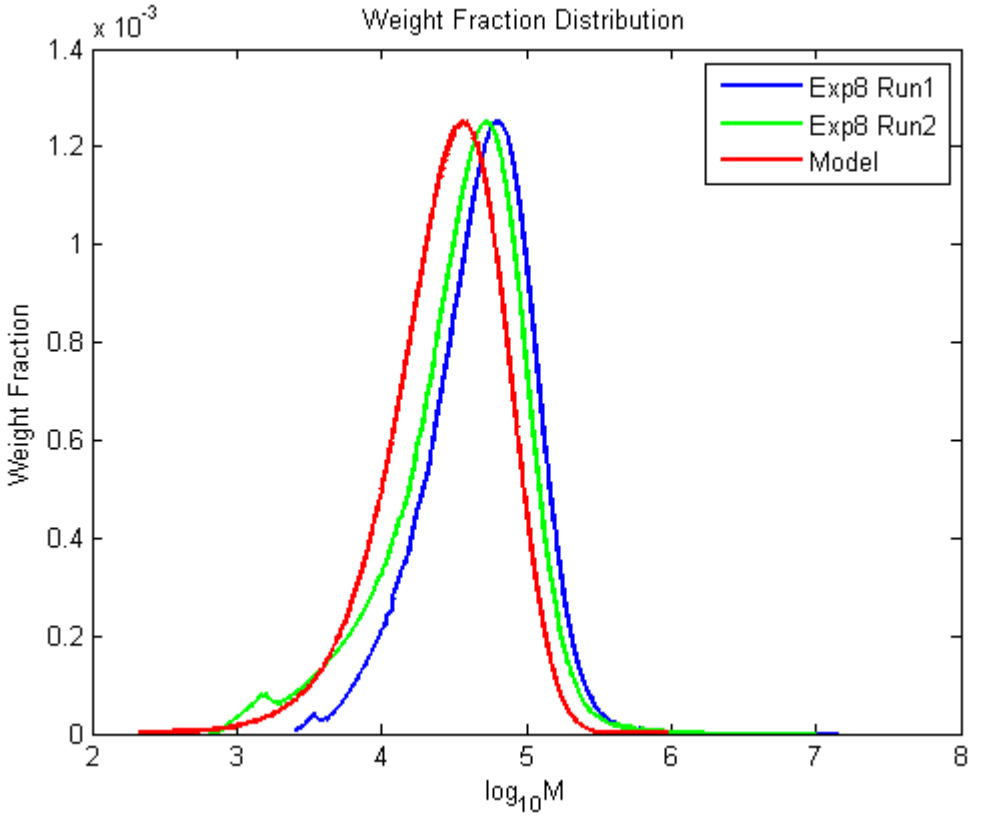
Weight Fraction Distribution
x 10^-3
Weight Fraction
log10M
Exp8 Run1
Exp8 Run2
Model

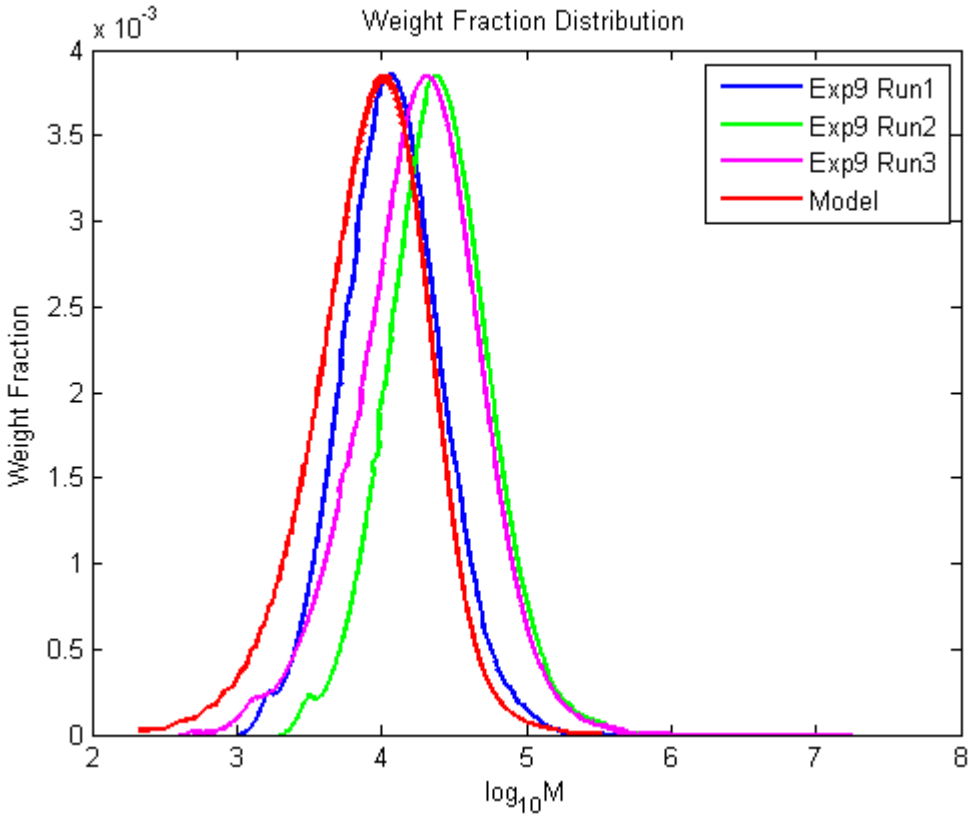
Weight Fraction Distribution
x 10^-3
Weight Fraction
log10M
Exp9 Run1
Exp9 Run2
Exp9 Run3
Model

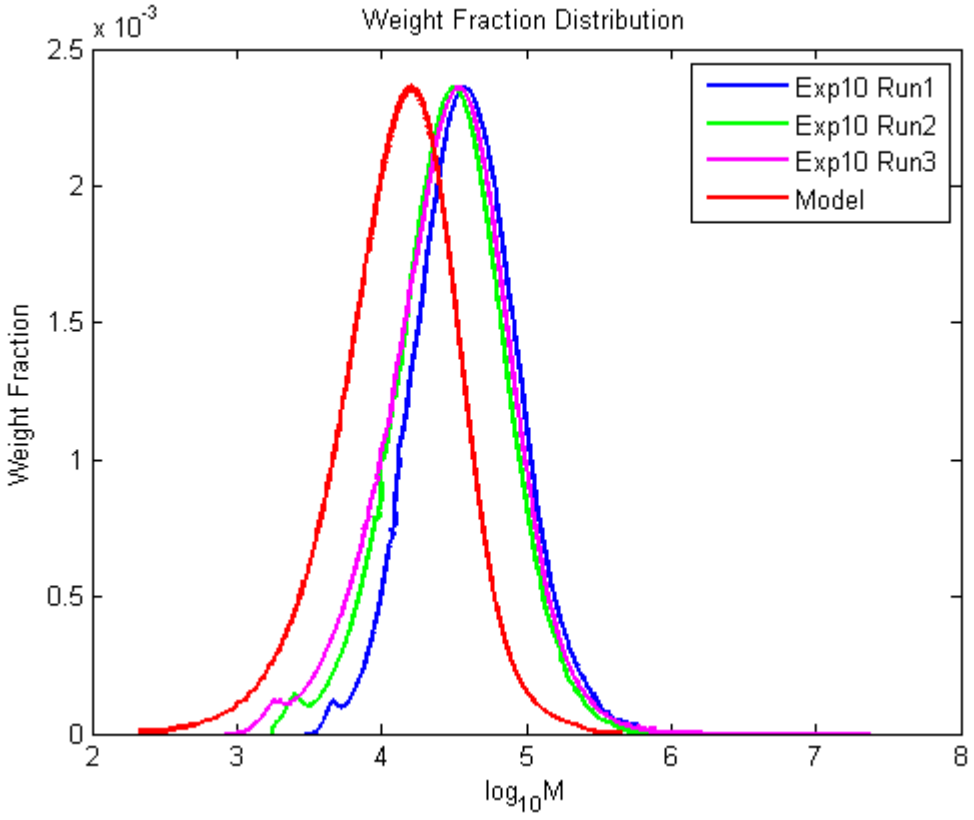
Weight Fraction Distribution
x 10^-3
Weight Fraction
log10M
Exp10 Run1
Exp10 Run2
Exp10 Run3
Model

Chapter 7. Bibliography

AMERICAN CHEMISTRY COUNCIL. History of Polymer and Plastics. Disponivel em: <http://plastics.americanchemistry.com/Education-Resources/Hands-on-Plastics/Introduction-to-Plastics-Science-Teaching-Resources/History-of-Polymer-and-Plastics-for-Students.html>. Acesso em: 14 maio 2014.

ASUA, J. M. **Polymer reaction engineering**. Oxford: Blackwell Publishing Ltd, 2007. 392 p.

BARNER-KOWOLLIK, C.; RUSSELL, G. T. Chain-length dependent termination in radical polimerization: Subtle revolution in tackling a long-standing challenge. **Progress in Polymer Science**, v. 34, p. 1211-1259, 2009.

BENSON, S. W.; NORTH, A. M. The Kinetics of Free Radical Polymerization under Conditions of Diffusion-controlled Termination. **Journal of the American Chemical Society**, v. 6, p. 935-940, 1962.

BERGER, K. C.; MEYERHOFF, G. Disproportionierung und kombination als abbruchmechanismen bei der radikalischen polymerisation von styrol, 1.Versuche mit 14C-markierten 2,2′-azoisobutyronitril. **Die Makromolekulare Chemie**, v. 176, n. 7, p. 1983-2003, 1975.

BERNE, B. J.; PECORA, R. **Dynamic Light Scattering:** With Applications to Chemistry, Biology, and Physics. [S.l.]: Courier Dover Publications, 2000. 24-33 p.

BOODHOO, K. V. K. Process Intensification: Spinning Disc Reactor for the Polymerization of Styrene. **Newcastle Upon Tyne University**, Newcastle Upon Tyne, 1999.

BRANDRUP, J.; IMMERGUT, E. H. **Polymer Handbook**. 3rd Edition. ed. Chichester: Wiley-Interscience, 1989.

BUBACK, M.; KUCHTA, F.-D. Termination kinetics of free-radical polymerization of styrene over an extended temperature and pressure range. **Macromolecular Chemistry and Physics**, 198, n. 5, 1997. 1455-1480.

BUDDE, U.; WULKOW, M. Computation of Molecular Weight Distributions for Free Radical Polymerization Systems. **Chemical Engineering Science**, v. 46, n. 2, p. 497-508, 1991.

CABRAL, P. A. et al. Free-radical solution polymerization of styrene in a tubular reactor—effects of recycling. **Polymer Engineering & Science**, v. 43, n. 6, p. 1163-1179, 2004.

CHAIMBERG, M.; COHEN, Y. Kinetic modeling of free-radical polymerization: a conservational polymerization and molecular weight distribution model. **Industrial & Engineering Chemistry Research**, v. 29, n. 7, p. 1152-1160, 1990.

CHIU, W. Y.; CARRATT, G. M.; SOONG, D. S. Computer model for the gel effect in free-radical polymerization. **Macromolecules**, v. 16, n. 3, p. 348-357, 1983.

CLAY, P. A.; GILBERT, R. G. Molecular Weight Distributions in Free-Radical Polymerizations. 1. Model Development and Implications for Data Interpretation. **Macromolecules**, v. 28, n. 2, p. 552-569, 1995.

COWIE, J. M. G.; ARRIGHI, V. **Polymers:** Chemistry and Physics of Modern Materials. 3rd. ed. Boca Raton: CRC Press, 2007. 520 p.

CROWLEY, T. J.; CHOI, K. Y. Control of molecular weight distribution and tensile strength in a free radical styrene polymerization process. **Journal of Applied Polymer Science**, v. 70, n. 5, p. 1017-1026, 1998.

CUTTER, L. A.; DREXLER, T. D. Simulation of the Kinetics of Styrene Polymerization. [S.l.]: American Chemical Society, 1982.

DEUFLHARD, P.; WULKOW, M. Computational treatment of polyreaction kinetics by orthogonal polynomials of a discrete variable. **IMPACT of Computing in Science and Engineering**, v. 1, n. 3, p. 269-301, 1989.

EDWIN, N. J. Characterization of Polymer Particles via Dynamic Light Scattering and Diffusion Ordered Spectroscopy Techniques. **Master thesis submitted to the LSU IGERT Program**, 2001.

FERNANDO, H. J. S. **Handbook of Environmental Fluid Dynamics**. Boca Raton: Taylor & Francis Group, v. II, 2013. 368 p.

FISCHER, J. P.; MÜCKE, G.; SCHULZ, G. V. Der Einfluß des Lösungsmittels auf die Teilreaktionen bei der radikalischen Polymerisation des Methylmethacrylates. **Berichte der Bunsengesellschaft für physikalische Chemie**, 73, n. 2, 1969. 154-163.

FLORENZANO, F. H.; STRELITZKI, R.; REED, W. F. Absolute, On-Line Monitoring during Polymerization Reactions. **Macromolecules**, v. 31, p. 7226-7238, 1998.

FONTOURA, J. M. R. et al. Monitoring and Control of Styrene Solution Polymerization Using NIR Spectroscopy. **Journal of Applied Polymer Science**, v. 90, p. 1273-1289, 2003.

FU, Y. et al. Atom-Transfer Radical Batch and Semibatch Polymerization of Styrene. **Macromolecular Reaction Engineering**, v. 1, n. 4, p. 425-439, 2007.

FULLIN, L. Solution Polymerization in a Millireactor - Master Thesis. **Universidade de Sao Paulo**, Sao Paulo, 2014.

GEAR, B. Backward differentiation formulas. **Scholarpedia**, 2007. Disponivel em: <http://www.scholarpedia.org/article/Backward_differentiation_formulas>. Acesso em: 21 maio 2014.

GOPALAN, M. R.; SANTHAPPA, M. Methyl ethyl ketone peroxide as an initiator in the polymerization of vinyl monomers. **Journal of Polymer Science**, v. 25, n. 110, p. 333-349, 1957.

HAMED, O.; MOMAN, A.; ABU-RAQABAH, A. **Catalyst Compositions for Polymerizing Olefins to Multimodal Molecular Weight Distribution Polymer, Processes for Production and Use of the Catalyst**. US 6784263, 31 ago. 2004.

HAMIELEC, A. E.; HODGINS, J. W.; TEBBENS, K. Polymer Reactors and Molecular Weight Distribution: Part II. Free Radical Polymerization in a Batch Reactor. **AIChE Journal**, v. 13, n. 6, p. 1087-1091, 1967.

HUI, A. W.; HAMIELEC, A. E. Thermal polymerization of styrene at high conversions and temperatures. An experimental study. **Journal of Applied Polymer Science**, v. 16, n. 3, p. 749-769, 1972.

INDIAN ACADEMY OF SCIENCES. Polymer Molecular Weight. Disponivel em: <http://www.ias.ac.in/initiat/sci_ed/resources/chemistry/MolWeight.pdf>. Acesso em: 14 maio 2014.

IWASAKI, T.; YOSHIDA, J.-I. Free Radical Polymerization in Microreactors. Significant Improvement in Molecular Weight Distribution Control. **Macromolecules**, 38, 2005. 1159-1163.

JACKSON, R. A.; SMALL, P. A.; WHITELEY, K. S. Prediction of molecular weight distributions in branched polymers. **Journal of Polymer Science - Part A Polymer Chemistry**, v. 11, n. 8, p. 1781-1809, 1973.

KIRSHENBAUM, G. S. **Polymer Science Study Guide**. 1st. ed. New York: Gordon and Breach Science Publishers, 1973.

KRICHELDORF, H. R.; NUYKEN, O.; SWIFT, G. **Handbook of Polymer Synthesis**. 2nd. ed. New York: Marcel Dekker, 2010.

LUCAS, E. F.; SOARES, B. G.; MONTEIRO, E. **Caracterização de Polímeros**. Rio de Janeiro: E-papers Serviços Editoriais, 2001. 366 p.

MAHABADI, H. K. Effects of chain length dependence of termination rate constants on the kinetics of free-radical polymerization. 1. Evaluation of an analytical expression relating the apparent rate constant of termination to the number-average degree of polymerization. **Macromolecules**, v. 18, n. 6, p. 1319-1324, 1985.

MAHABADI, H. K.; O'DRISCOLL, K. F. Absolute Rate Constants in Free-Radical Polymerization. III. Determination of Propagation and Termination Rate Constants for Styrene and Methyl Methacrilate. **Journal of Macromolecular Science: Part A - Chemistry**, v. 11, n. 5, p. 967-976, 1977.

MARTEN, F. L.; HAMIELEC, A. E. **American Chemical Society Symposium Series**, v. 104, p. 43, 1979.

MASCHIO, G.; MOUTIER, C. Polymerization Reactor: The Influence of "Gel Effect" in Batch and Continuous Solution Polymerization of Methyl Methacrylate. **Journal of Applied Polymer Science**, v. 37, p. 825-840, 1989.

MASSOUD, M. Nonlinear Systems of Ordinary Differential Equations. In: MASSOUD, M. **Differential Equations**. [S.l.]: California State University.

MATHWORKS. Documentation Center - ode15s, 2014. Disponivel em: <http://www.mathworks.com/help/matlab/ref/ode15s.html>. Acesso em: 04 jun. 2014.

MATYJASZEWSKI, K.; DAVIS, T. P. **Handbook of Radical Polymerization**. Hoboken: John Wiley & Sons, 2003.

MELLONI, E. Rigorous Computation of Free Radical Polymerization Kinetics. **Universidade de São Paulo**, 2014.

MILLER-CHOU, B. A.; KOENIG, J. L. A review of polymer dissolution. **Progress in Polymer Science**, v. 28, n. 8, p. 1223-1270, 2003.

NAJAFI, M. et al. An exhaustive study of chain-length-dependent and diffusion-controlled free radical and atom-transfer radical polymerization of styrene. **Journal of Polymer Research**, v. 18, n. 6, p. 1539-1555, 2011.

ODIAN, G. **Principles of Polymerization**. New York: John Wiley & Sons, 2004.

PLADIS, P.; KIPARISSIDES, C. A comprehensive model for the calculation of molecular weight-long-chain branching distribution in free-radical polymerization. **Chemical Engineering Science**, v. 53, n. 18, p. 3315-3333, 1998.

REED, W. F. Background and Principles of Automatic Continuous Online Monitoring of Polymerization Reactions (ACOMP). In: REED, W. F.; ALB, A. M. **Monitoring Polymerization Reactions**. Hoboken: John Wiley & Sons, 2014. p. 473.

ROSS, R. T.; LAURENCE, R. L. Gel effect and free volume in the bulk polymerization of methyl methacrylate. **AIChe Symposium Series**, v. 160, p. 72-74, 1976.

SALDIVAR-GUERRA, E.; VIVALDO-LIMA, E. **Handbook of Polymer Synthesis, Characterization, and Processing**. Hoboken: John Wiley & Sons, 2013. 644 p.

SALDÍVAR-GUERRA, E. et al. Returning to Basics: Direct Integration of the Full Molecular-Weight Distribution Equations in Addition Polymerization. **Macromolecular Theory and Simulations**, v. 19, p. 151-157, 2010.

SARMORIA, C.; ASTEASUAIN, M.; BRANDOLIN, A. Prediction of molecular weight distribution in polymers using probability generating functions. **The Canadian Journal of Chemical Engineering**, v. 90, n. 2, p. 263-273, 2012.

SCHMIDT, A. D.; RAY, W. H. The Dynamic Behavior of Continuous Polymerization Reactors - Isothermal Solution Polymerization in a CSTR. **Chemical Engineering Science**, v. 36, p. 1401-1410, 1981.

SCHULTZ, V. G.; HARBORTH, G. Über den mechanismus des explosiven polymerisationsverlaufes des methacrylsäuremethylesters. **Die Makromolekulare Chemie**, v. 1, n. 1, p. 106-139, 1947.

SHAMPINE, L. F.; REICHELT, M. W. The MATLAB ODE Suite. **SIAM Journal on Scientific Computing**, v. 18, n. 1, p. 1-22, 1997.

SKOOG, D. A.; HOLLER, F. J.; NIEMAN, T. A. **Principles of instrumental analysis**. 6th. ed. Belmont: Thomson, Brooks/Cole, 2007. 1039 p.

SMITH, G. B.; RUSSELL, G. T.; HEUTS, J. P. A. Termination in Dilute-Solution Free-Radical Polymerization: A Composite Model. **Macromolecular Theory and Simulations**, 12, 2003. 299-314.

SPIJKER, M. N. Stiffness in numerical initial-value problems. **Journal of Computational and Applied Mathematics**, v. 72, p. 393-406, 1996.

TOBOLSKY, A. V.; BAYSAL, B. A review of rates of initiation in vinyl polymerization: Styrene and methyl methacrylate. **Journal of Polymer Science**, v. 11, n. 5, p. 471-486, 1953.

TULIG, T. J.; TIRRELL, M. Toward a Molecular Theory of the Trommsdorff Effect, v. 14, p. 1501-1511, 1981.

TURTON, R. **Analysis, Synthesis and Design of Chemical Processes**. [S.l.]: Prentice Hall, 2008. ISBN 3.

WHITELEY, K. S.; GARRIGA, A. Derivation of continuous molecular weight distributions from the generating function. **Computational and Theoretical Polymer Science**, v. 11, n. 4, p. 319-324, 2001.

ZAMMIT, M. D. et al. Evaluation of the Mode of Termination for a Thermally Initiated Free-Radical Polymerization via Matrix-Assisted Laser Desorption Ionization Time-of-Flight Mass Spectrometry. **Macromolecules**, v. 30, n. 7, p. 1915-1920, 1997.

ZHANG, X. et al. Microreactors as a tool for chemical research. **Chemistry Today**, v. 24, n. 2, p. 43-45, 2006.